Extracellular redox sensors control the protein secretion stress response in *Streptomyces*

Thomas C. McLean[1,2*], Ainsley D. M. Beaton[1,2*], Neil A. Holmes [1,2], Carlo Martins[2,3], Gerhard Saalbach[2,3], Govind Chandra[1,2], Sibyl F.D. Batey[1], Jana China[1], Barrie Wilkinson[1,2] and Matthew I. Hutchings[1,2]

[1]Department of Molecular Microbiology, John Innes Centre, Norwich, Norwich Research Park, NR4 7UH, UK.
[2]The Centre for Microbial Interactions, Norwich, Norwich Research Park, NR4 7UG, UK.
[3]Department of Biochemistry and Metabolism, Proteomics Facility, John Innes Centre, Norwich, Norwich Research Park, NR4 7UH, UK.

Correspondence: barrie.wilkinson@jic.ac.uk and matt.hutchings@jic.ac.uk

[*] These authors contributed equally to this work

SUMMARY

Translocating unfolded polypeptides across membranes is essential in all domains of life and in bacteria requires the conserved Sec machinery and ATP. Bacterial Sec substrates fold outside the cell and often use DsbA-catalysed disulfide bond formation between cysteines to ensure correct folding. Extracellular protein misfolding triggers a stress response that involves production of dual function HtrA-family chaperone/proteases. In Gram-negative bacteria this is called the envelope stress response and in Gram-positive bacteria the secretion stress response, but the exact signals sensed by bacteria to trigger these stress responses are not well understood. In *Streptomyces* bacteria the secretion stress response is mediated by the CutRS and CssRS two-component systems which control the levels of four conserved HtrA-family chaperones. Here we show that the CutS sensor kinase contains two conserved cysteine residues in its extracellular sensor domain that control CutS activity. CssS also has two conserved and invariant cysteines in its sensor domain, and we propose that CutS and CssS detect the extracellular redox state and work together to ensure secreted proteins fold correctly in the fluctuating soil environment. Further analysis of ~12,800 genomes indicated that 98.9% of strains across all bacterial classes have at least one sensor kinase with two or more extracellular cysteine residues, suggesting that extracellular redox sensing by two-component systems is widespread in bacteria.

INTRODUCTION

Bacteria typically secrete around 10% of their total cellular proteins and most of these are translocated across the cytoplasmic membrane as unfolded polypeptides via the highly conserved general secretory (Sec) pathway. During translocation, hydrophobic Sec substrates are inserted into the membrane while globular proteins are released to fold in the periplasm (diderm bacteria) or extracellular environment (monoderm bacteria). Many Sec substrates contain even numbers of cysteine residues which help them fold via DsbA-catalysed disulfide bond formation as they emerge from the extracellular face of the membrane [1,2]. However, these systems can fail and the accumulation of misfolded proteins on the extracellular face of the cell membrane triggers the envelope stress response in *E. coli* and the secretion stress response in *Bacillus* and *Streptomyces* species [3,4]. These responses are typically mediated by two-component systems (TCS) which are generally composed of a membrane bound sensor kinase (SK) which detects and responds to environmental stimuli via phosphorylation of its cognate response regulator (RR) which can modulate target gene expression by binding to specific DNA sequences[5,6]. In the case of secretion stress responses, TCS control the production of High temperature requirement A (HtrA) family proteins that have dual chaperone/protease activities [7–9]. In *E. coli*, the CpxAR two-component system senses protein misfolding and controls the levels of the HtrA-family protein DegP in the periplasm, while in *Bacillus subtilis* the homologous CssRS controls the production of HtrA and HtrB[10–12]. *Streptomyces* species encode four HtrA-family proteins: HtrA1, HtrA2, HtrA3 and HtrB and their production is controlled by two conserved TCS. CssRS activates the production of HtrA1, HtrA2 and HtrB while another conserved two-component system named CutRS activates production of HtrA3 and represses the production of HtrB[8,13].

In aerobic Actinobacteria, exported proteins average 2.2 cysteines per protein and 60% of secreted proteins contain even numbers of cysteines[14]. In the model organism *Streptomyces venezuelae*, this figure is 74%, suggesting that disulfide bond formation plays a key role in protein maturation outside the cell. Consistent with this, *Streptomyces* species encode four conserved thiol oxidoreductases (TDORs) named DsbA, DsbB, DsbC, and DsbD, which oxidise the thiol groups of cysteine residues to form disulfide bonds in Sec-secreted proteins [15]. DsbA is a membrane tethered lipoprotein, [16] DsbB and DsbD are predicted to be integral membrane proteins, and DsbC is predicted to be a secreted protein. In all four cases, their active sites are predicted to localise to the extracellular face of the membrane, where they contribute to disulfide bond formation and protein folding [2,15]. Loss of any one of these TDORs in *Streptomyces lividans* results in reduced activity of α-amylase, a secreted enzyme which requires disulfide bond formation to form an active protein outside the cell [15]. Misfolding of α-amylase triggers the activation of CssRS which then activates the expression of *htrA1*, *htrA2* and *htrB*, with all three required to restore the α-amylase to full functionality [8].

In this work we set out to understand the conserved CutRS system, the signals it senses and the target genes it controls. We chose to do this in the fast-growing *S. venezuelae* which has recently emerged as an ideal model organism for studying *Streptomyces* growth and development [17].

Here we report that the core regulon of the DNA binding RR CutR, shared between *Streptomyces coelicolor* and the distantly related *S. venezuelae*, contains only two target genes: *htrA3* and *htrB,* providing further evidence that its cognate SK CutS is dedicated to sensing protein misfolding outside the cell. Alignment of >100 *Streptomyces* CutS homologues revealed that two invariant cysteine residues are the only conserved residues in their extracellular sensor domains and we show that they are required for the activation of CutRS suggesting this system monitors disulfide bond formation outside the cell. Analysis of the extracellular domains of all bacterial SKs across 12,799 species revealed that 99% encode at least one SK with two or more extracellular cysteines. We tentatively propose that extracellular redox sensing by SKs is likely to be widespread across the bacterial kingdom.

RESULTS

Deletion of *cutRS* affects growth and antibiotic production in *S. venezuelae*

Previous work in *S. coelicolor* suggested that the CutRS two-component system co-ordinates the protein secretion stress response via direct regulation of the extracellular chaperone/protease genes *htrA3* and *htrB* by the RR CutR. CutR binding sites were also found upstream of 83 other genes with no obvious roles in protein secretion[13]. To further analyse the function of CutRS we deleted the *cutRS* operon in *S. venezuelae* and found that the Δ*cutRS* mutant has a striking phenotype when grown on yeast peptone + D-glucose (YPD) agar. The mutant exhibits increased antibacterial activity and accelerated growth (Figures 1, 2A and 2B). Further analysis revealed that the Δ*cutRS* strain forms 10 fold more biomass than the wild-type (WT) strain on YPD agar. This was not restricted to YPD medium; a similar increase in biomass was observed in the Δ*cutRS* strain relative to WT on MYM agar, but again only in the presence of glucose (Figure 2B). This growth coincides with the rapid consumption of glucose from the growth medium (Figure 2C). Consistent with this, in the absence of glucose (YP agar) we observed no difference in phenotypes between the wild-type and Δ*cutRS* strains (Figures 1A, 2A and 2B).

Previous work in *S. coelicolor* and *S. lividans* revealed that deletion of the *cutRS* operon leads to an increase in production of the blue-pigmented antibiotic actinorhodin [13,18] which is similarly dependent on the presence of glucose in the growth media [19]. We challenged the *S. venezuelae* WT and Δ*cutRS* strains with a range of antimicrobial indicator organisms using agar plate bioassays. When these strains were challenged with *B. subtilis* in the absence of glucose (YP agar) both exhibited a small zone of inhibition (Figure 1A). In the presence of glucose (YPD agar) this bioactivity was lost in the WT strain, consistent with general inhibition of antibiotic biosynthesis via glucose-mediated carbon catabolite repression [20]. Strikingly however, the *S. venezuelae* Δ*cutRS* strain exhibited a substantially larger zone of inhibition in

the presence of glucose (YPD agar) when challenged with *B. subtilis* (Figure 1A). This suggests that glucose induces antibiotic overproduction in the *S. venezuelae* Δ*cutRS* strain, concurrent with our previous observations in *S. coelicolor* [13]. This is unusual because glucose typically represses antibiotic production in *Streptomyces* species[21,22].

S. venezuelae is known to produce the antibiotics chloramphenicol and jadomycin which both have activity against *B. subtilis.* We deleted both the chloramphenicol and jadomycin biosynthetic gene clusters in *S. venezuelae* resulting in strain M1702. When challenged, M1702 was incapable of inhibiting *B. subtilis* growth suggesting the inhibition was due to either chloramphenicol or jadomycin (Figure 1A). To determine if the activity was due to chloramphenicol, we challenged *S. venezuelae* WT and Δ*cutRS* strains with a chloramphenicol resistant strain of *B. subtilis.* Whilst the *S. venezuelae* Δ*cutRS* strain displayed a slight zone of inhibition, it was significantly reduced from the WT strain, confirming that the bioactivity was largely due to chloramphenicol production (Figure 1B). Finally, we used ethyl acetate to extract chloramphenicol from the agar of YPD plates cultured with the *S. venezuelae* WT and Δ*cutRS* strains. HPLC analysis confirmed that the Δ*cutRS* strain produced ~3 fold more chloramphenicol than the WT in the presence of glucose and we conclude that this is responsible for the increased antibacterial activity of this strain (Figure 1C).

Identifying CutR target promoters and binding sites in *S. venezuelae*

TCS mediate gene transcription through the RR, in this case CutR. To determine the regulon of genes under the control of CutR, we complemented the *S. venezuelae* Δ*cutRS* strain with a modified *cutRS* operon encoding the wild-type CutS SK and C-terminally 3xFlag-tagged CutR. Subsequently we cultured both the WT and Flag-tagged strains on YP and YPD a fgar and performed ChIP-seq using monoclonal α-Flag antibodies. Analysis of the sequencing data (accession number GSE225370) revealed one significantly enriched target in the Flag-tagged CutR strain grown in the absence of glucose (YP agar), which is upstream of the *cutRS* operon. However, 10 sites of enrichment were identified for the strains grown in the presence of glucose (YPD agar, Table 1). This included peaks upstream of both the *htrA3* and *htrB* genes, which are also CutR targets in *S. coelicolor* (Figure 3A)13, and upstream of a putative cell wall amidase gene *vnz_08815* which was also highly enriched in this dataset.

To precisely define the CutR binding site we expressed and purified hexahistidine-tagged CutR protein for use in a DNA footprinting technique called Reuseable DNA Capture Technology surface plasmon resonance (ReDCaT SPR) [23]. We used tiled, double stranded oligonucleotide probes to span the promoter sequences of *htrA3* and *vnz_08815* and SPR was then used to measure the binding affinity of purified CutR to these probes. A preliminary scan was performed on all probes to identify the core binding region and the bound probes were then subjected to 2 bp truncations to identify the minimal CutR binding sites (Figure 3B). At the *htrA3* promoter, CutR binds to the sequence TATATAAA, and at the *vnz_08815* promoter CutR binds to the sequence TAAATAAA (Figure 3B). From the full comparison of all putative CutR binding sites we were able to define the CutR consensus binding sequence as TAWATAAA.

CutR is both a transcriptional activator and repressor

Having identified the CutR binding sites at all its target promoters (Table 1), we cross-
150 referenced it with publicly available *S. venezuelae* transcript start site (TSS) data available at http://streptomyces.org.uk[24]. The DNA recognition site at the *htrB* promoter is located 17 bp upstream of the TSS, whilst at the *htrA3* promoter, it is positioned 62 bp upstream (Table 1 and Figure 3A). The binding site position of a transcriptional regulator relative to the TSS typically determines its mechanism of action, i.e., activation or repression [25]. Thus, CutR binding 17 bp upstream of the *htrB* TSS would likely interfere with RNA polymerase binding resulting in transcriptional repression [26,27]. Binding upstream of the -35 RNA polymerase binding site, as is the case with the *htrA3* promoter, is more likely to result in transcriptional activation via positive interaction between CutR and the bound RNA polymerase [27–29]. Next we used quantitative tandem mass tag (TMT) proteomics to examine the effects of removing
160 *cutRS* on the production of CutR-dependent gene products. We detected six of the ten CutR-dependent gene products (Table 1) and these data indicate that CutR activates the production of HtrA3 (8 fold increase) and the putative cell wall amidase Vnz_08815 (2.5 fold increase), consistent with the CutR binding site positions at their promoters (Figure 4, Table 1, and Supplementary Table 1). CutR represses production of HtrB (19 fold decrease) which is also consistent with the CutR binding site position which must occlude RNA polymerase binding (Figure 3A). The production of other target proteins detected in this experiment were not significantly affected by the loss of CutRS. This could either be because the encoding genes are not regulated by CutR, or CutR does not bind and repress under the growth conditions used in this experiment, or the genes are subject to more complex regulation (Table 1).

170

Table 1. Gene promoters with CutR binding sites that are enriched in the ChIP-seq dataset. The binding site positions are given relative to the transcript start sites (TSS). The DNA sequences of the CutR binding sites are shown, two of which (*htrA3* and *vnz_08815*) were verified *in vitro* using ReDCaT SPR (Figure 3).

Gene	Predicted function	CutR binding site relative to TSS	Binding site sequence	Predicted effect	Protein abundance (WT/Δ*cutRS)*
vnz_06385	Acyl coA dehydrogenase	+21	TAATTAAA	Repression	0.795
vnz_06390	TetR-family regulator	+28	TAATTAAA	Repression	0.947
vnz_08815	Cell wall amidase	-69	TAAATAAA	Activation	2.56
vnz_12615	Membrane protein	-4	TACATAAA	Repression	ND
htrA3	Quality control protease	-62	TATATAAA	Activation	8.134
htrB	Quality control protease	-17	CATATAAA	Repression	0.053
vnz_29845	NAD(P)/FAD-dependent oxidoreductase	-28	CAAATAAA	Repression	0.707
vnz_33990	Beta mannosidase	-21	TAAGTAAA	Repression	0.747
vnz_33995	Sugar binding protein for ABC transport	+1	TAAGTAAA	Repression	0.977

CutS activity is controlled by two conserved cysteines in its extracellular sensor domain The conservation of *htrA3* and *htrB* as CutR targets in the distantly related species *S. coelicolor* and *S. venezuelae* supports the hypothesis that CutRS plays a role in the protein secretion stress response. This further implies that CutRS complements the function of CssRS, which activates the expression of *htrA1*, *htrA2* and *htrB*, but not *htrA3* [8]. We thus set out to investigate how the extracellular sensor domain, between the two predicted transmembrane helices of CutS might detect defects in protein folding on the outside of the cell. We first aligned the extracellular sensor domains of >100 CutS proteins taken from complete, published *Streptomyces* genome sequences to look for conserved residues or motifs. This analysis identified two cysteine residues that are conserved across every CutS sensor domain (Supplementary Figure 3). Furthermore, analysis of all proteins encoded in *S. venezuelae* with a Sec signal sequence revealed that 74% contain two or more cysteines that likely form disulfide bonds to help them fold [1]. We thus hypothesised that CutS is monitoring the redox status of the extracellular environment as a proxy for correct disulfide bond formation in Sec-translocated proteins. Given the conservation of the two cysteine residues we reasoned that this could be via the making or breaking of a disulfide bond in the CutS extracellular sensor domain.

Modelling of the *S. venezuelae* CutS extracellular sensor domain using AlphaFold indicated that these cysteines likely sit within 5Å of each other, the distance required to form disulfide bonds (Supplementary Figure 4). To test this, we designed a CutS variant where these residues were replaced with serine (CutS(C85S,C103S)) and introduced it into the *S. venezuelae* WT and Δ*cutRS* strains. This restored a WT growth phenotype to the Δ*cutRS* mutant (Figure 5A) which suggests the CutS(C85S,C103S) variant is active. However, previous work on the VanRS TCS demonstrated that it is possible for loss of a SK to render its cognate RR constitutively active [30]. To discount this possibility, we introduced individual copies of either *cutS* or *cutR* under the control of the *ermE** promoter into the Δ*cutRS* mutant, but neither restored the WT phenotype, confirming that CutS is required for CutR activity. To further investigate the activity of the CutS(C85S,C103S) variant we used qRT-PCR to measure the expression of the CutR target genes *htrA3* and *htrB* in the WT, Δ*cutRS* and CutS(C85S,C103S) strains (Figure 5B). The expression of *htrA3* was higher in the strain harboring the CutS(C85S,C103S) variant compared to the WT strain, while the expression of *htrB* was reduced (Figure 5B) which is consistent with CutS(C85S,C103S) activating CutR which then directly activates the transcription of *htrA3* and represses *htrB*. Thus, we conclude that replacing the two extracellular sensor domain cysteines with serine residues results in a constitutively active CutRS system which supports the hypothesis that an inability to form disulfide bonds outside the cell activates CutRS and triggers the secretion stress response.

The wild-type phenotype is recovered by the deletion of *cssRS* in the Δ*cutRS* background

This work and previous reports have shown that the secretion stress response in *Streptomyces* species is controlled by the CssRS and CutRS TCS which together control the expression of *htrA1*, *htrA2*, *htrA3* and *htrB* in *Streptomyces* species [8,13]. Although the CssR

regulon has not yet been defined, electrophoretic mobility shift assays alongside qRT-PCR were used previously in *S. lividans* (a very close relative of *S. coelicolor*) to show that CutR directly activates expression of *htrA1*, *htrA2* and *htrB*, but not *htrA3* [8], Instead, the expression of *htrA3* is directly activated by CutR, which also represses the expression of *htrB* in *S. coelicolor* and *S. venezuelae* [13]. We attempted to replicate the Δ*cutRS* phenotype by deleting *htrA3* and overexpressing *htrB* in the same background (Supplementary Figure 2), but this did not result in the phenotypic change on YPD that we observed with Δ*cutRS*. We thus reasoned that the CssRS system might be compensating for the loss of CutRS. To further investigate the interplay of CssRS and CutRS we made single and double Δ*cssRS* and Δ*cutRS* mutants of *S. venezuelae* and observed their phenotypes on YP and YPD agar. In the absence of glucose (YP agar) all the WT, Δ*cssRS*, Δ*cutRS* and Δ*cssRS*Δ*cutRS* strains all displayed the same phenotype (Figure 6). On YPD agar, growth is reduced in the WT strain by the addition of glucose to the medium but the Δ*cutRS* mutant consumes the glucose and reverts to a phenotype more like that observed on YP agar (Figures 1 and 5). Deletion of *cssRS* in the WT background has no obvious effect on growth on either YP or YPD agar, but deletion of *cssRS* in the Δ*cutRS* mutant restores the WT phenotype to the *ΔcutRS* mutant growing on YPD agar, suggesting that the altered growth of the Δ*cutRS* mutant on YPD is dependent on CssRS (Figure 6). Proteomics analysis of the WT and Δ*cutRS* strains revealed that the levels of CssRS are increased 5-fold, and as previously discussed, HtrB levels (activated by CssR and repressed by CutR) are increased 20-fold in the absence of *cutRS*. The *htrB* and *cssRS* genes are located adjacent to each other and likely form an operon under the direct control of both CutR and CssR. Overproduction of HtrB could be due to the loss of CutR repression in the mutant strain combined with the overproduction of CssRS, with CssR further activating *htrB* expression. A future challenge will be to define the CssR regulon and determine how deletion of *cssRS* complements Δ*cutRS*.

Extracellular redox sensing is likely conserved across bacteria

There are 15 TCS that are conserved across *Streptomyces* species, with each species encoding additional TCS as well as orphan RRs and SKs [31–33]. Following our analysis of the CutS sensor domain we also identified two conserved cysteine residues in the extracellular domains of CssS (Supplementary Figure 5). To our knowledge, CutS is the first example of a extracellular redox sensing SK in bacteria, but our analysis suggests CssS activity may also be controlled by disulfide bond formation. Of the 15 conserved TCS in *Streptomyces* spp., only CutS and CssS have two conserved extracellular cysteines.

To investigate how widespread this might be in the bacterial kingdom, we analysed 12,799 high-quality bacterial genomes, identifying 348,633 proteins predicted to function as SKs. Using DeepTMHMM [34] we predicted the transmembrane helices for all the SKs and then used this information to identify the putative sensor domains of these proteins and quantify the number of cysteine residues present in these extracellular domains. We observed that 98.9% of all the bacterial strains encode at least one SK with two or more cysteines in its extracellular sensor domain (Figure 7A) and these data support our hypothesis that

extracellular redox sensing by SKs via extracellular disulfide bond formation is likely conserved across bacteria.

260 Next, we examined the conservation of the CutS and CssS SKs beyond the genus *Streptomyces*. Reciprocal BLAST searches in 2,936 bacterial reference genomes revealed that 39% encoded a CutS homologue and 27% encoded a CssS homologue. Of the 2,936 genomes examined, 53% encode at least one of these two SKs and 12% encode both CutS and CssS. However, further inspection of the amino acid sequences of these homologues revealed that only 6.9% of CutS and 4.8% of CssS homologues contain two or more cysteines in their extracellular domains. Phylogenetic analysis using a maximum likelihood tree based on RpoB revealed a broad distribution of these homologues across bacterial taxa (Figure 7B). The presence of both CutS and CutR with two extracellular cysteines was universally conserved across all tested *Streptomyces* strains, with only three additional genomes, all from
270 actinobacteria, also containing both. This may reflect the fact that actinobacteria are more likely to use disulfide bond formation as a mechanism to fold their secreted proteins [14]. Taken together, our findings suggest that the proposed mechanism of extracellular redox state sensing via cysteine residues in the extracellular sensor domains of SKs might be important throughout the bacterial kingdom. This function is likely performed by a variety of different SKs, with CutS and CssS being largely restricted to the genus *Streptomyces*.

DISCUSSION

In this work we demonstrated that loss of the highly conserved CutRS TCS from *S. venezuelae* results in a drastic change in both growth and antibiotic production. To understand the
280 underlying mechanism(s) behind these changes we first defined the *S. venezuelae* CutR regulon. This identified two CutR targets that are conserved between *S. venezuelae* and the distantly related *S. coelicolor;* these are the *htrA3* and *htrB* genes which encode for two high temperature requirement A (HtrA) family proteases. In *S. venezuelae*, CutR represses *htrB* and activates *htrA3.* CutR also activates one other gene, *vnz_08815*, which is predicted to encode a cell wall amidase of unknown function. Using ReDCaT SPR with purified CutR protein we identified a consensus CutR binding sequence at the *htrA3* and *vnz_08815* promoters (TAWATAAA) that was subsequently identified at five additional promoters enriched in the CutR ChIP-seq dataset, completing the *S. venezuelae* CutR regulon. We also showed that the location of the CutR binding sequence in these promoters is indicative of the transcriptional
290 activity of CutS, either activation or repression, depending on its distance from the TSS. The activity of CutR was confirmed using TMT proteomics where, in the absence of *cutRS*, we observed an increase in the levels of HtrB and decrease in HtrA3.

Given that CutRS coordinates the expression of two of the four conserved *htrA*-like genes in *S. venezuelae* and *S. coelicolor,* we conclude that CutRS controls the secretion stress response, alongside the CssRS TCS [8,10]. The CssR regulon has not been defined, but it was previously demonstrated that CssR directly activates *htrA1*, *htrA2* and *htrB* expression while having no effect on *htrA3* [11]. Thus, CutRS and CssRS have opposite effects on *htrB* and

exclusively activate one or two of the four *htrA*-family genes. HtrA family proteins assist extracellular protein folding in both Gram-negative and Gram-positive bacteria and degrade
300 misfolded proteins outside the cell that cannot be rescued [35]. CssRS is conserved in Gram-positive bacteria and is homologous to the envelope stress sensing two-component system CpxAR in *E. coli*. Bioinformatics analysis revealed that CutRS and CssRS are conserved across *Streptomyces* species and most genomes within the phylum Actinobacteria encode either CssRS or CutRS. Homologues are also present in a diverse range of other bacterial phyla (Figure 7).

The folding of secreted proteins typically involves disulfide bond formation and the formation of these bonds is catalysed by DsbA-family proteins which are the primary disulfide bond donors on the extracellular face of the cytoplasmic membrane [36]. The discovery that the sensor domain of CutS contains two conserved cysteine residues implied a role in sensing
310 extracellular protein folding and by measuring the effects on *htrA3* and *htrB* expression in the CutS(C85S,C103S) producing strain, we confirmed that if a disulfide bond cannot form in the CutS sensor domain it activates the protein, leading to higher expression of *htrA3* and stronger repression of *htrB*.

Intriguingly, the CssS extracellular sensor domain also contains two conserved cysteine residues, and we found that CutS and CssS are the only conserved *Streptomyces* SKs to contain two extracellular cysteines. This suggests that CssS also senses disulfide bond formation via the making or breaking of a disulfide bond in its extracellular domain and this will be investigated in future work. Given that *cssRS* is overexpressed in the Δ*cutRS* mutant and deletion of *cssRS* in the Δ*cutRS* background restored the Δ*cutRS* mutant to WT growth,
320 we hypothesise that CssRS and CutRS play opposing roles in the monitoring and control of extracellular protein folding. Further work is required to fully define the CssR regulon, to untangle the complex interplay between CssRS and CutRS and to understand the roles of HtrA1, HtrA2, HtrA3 and HtrB.

To the best of our knowledge this is the first time an exact sensing mechanism has been described for a secretion/envelope stress sensing signal transduction system in bacteria. *Streptomyces* species are ubiquitous in soil and in the plant rhizosphere and endosphere [37] and protein secretion plays an essential role in breaking down complex polymers so they can be used as carbon and nitrogen sources for growth [37]. These soil bacteria must rapidly adapt to changing oxygen levels and survive under microaerobic and anaerobic conditions and we
330 propose that, as depicted in Figure 8 CutS senses oxygen availability, which is required for disulfide bond formation. In the absence of oxygen, disulfide bonds do not form, and this results in the accumulation of misfolded proteins on the extracellular face of the cytoplasmic membrane. The failure to form a disulfide bond in the sensor domain of CutS under these conditions activates the CutRS system, resulting in elevated levels of HtrA3, which acts to degrade or rescue misfolded proteins.

Sensing extracellular oxygen via disulfide bond formation is not unprecedented. For example, the Gram-negative bacterial genus *Shewenella* contains an MtrABC porin-cytochrome complex that allows it to shuttle electrons across the outer membrane under

anoxic conditions [38]. In this system the periplasmic subunit MtrC has a conserved CX_8C motif
340 that forms a redox active disulfide bond on the cytochrome surface. This disulfide only forms in the presence of oxygen and allows the bacteria to sense oxygen levels and reduce the levels of reactive oxygen species that would otherwise be formed by extracellular electron transfer under aerobic conditions [39]. In *Pseudomonas aeruginosa*, the activity of the periplasmic protein YfiR has four redox active cysteines, two of which form a disulfide bond under oxidative conditions. YfiR has been proposed to modulate the diguanylate cyclase activity the transmembrane protein YfiN in response to anoxia [40].

The widespread conservation of SKs with extracellular cysteine residues across bacterial phyla further suggests that extracellular redox and/or oxygen sensing is a fundamental aspect of bacterial stress responses. Future research into these systems could
350 uncover novel regulatory mechanisms governing protein secretion and stress adaptation-induced virulence in diverse species.

METHODS

Growth media and supplements

Protocols for culturing and genetically manipulating *Streptomyces* species are all freely available from http://actinobase.org [41]. Strains were grown in the following media (per L volume): Yeast Peptone (YP) agar (10 g yeast extract, 20 g bacto-peptone, 20 g agar); YPD (YP + D-glucose) agar (YP agar with the addition of 100 ml of a 40% filter-sterilised D-glucose); 2xYT (16 g tryptone, 10 g yeast extract, 5 g NaCl); SFM agar (20 g soy flour, 20 g mannitol, 20
360 g agar); lysogeny broth (LB) (10 g tryptone, 5 g yeast extract, 10 g NaCl) and LB soft agar (LB with the addition of 20 g agar). When appropriate, the media was supplemented with antibiotics at the following concentrations: hygromycin (50 µg/ml), apramycin (50 µg/ml) and nalidixic acid (25 µg/ml). NaCl was excluded from LB when hygromycin was used for selection.

Strains, plasmids, and primers

The bacterial strains, plasmids and primers used or generated in this study are listed in Supplementary Tables 2, 3 and 4, respectively.

Strain generation

370 Deletion mutants were complemented using the native gene and promoter cloned into the phage integrative vector pSS170 [41] using Gibson Assembly. Overexpression strains were generated by cloning the gene(s) of interest into pIJ10257 [28] using Gibson Assembly. CRISPR mediated gene deletions were carried out using pCRISPomyces2 as per the protocol described by Cobb et al.[42]. In all cases the resulting construct was then used to transform *E. coli* ET12567/pUZ8002 [43,44] and conjugated into the mutant strains as follows. Single colonies of ET12567/pUZ8002 containing the complementation construct were inoculated into 10 ml LB with appropriate selection and incubated overnight at 37°C with shaking at 220 rpm. The overnight culture was sub-cultured 1:100 in 50 ml LB with appropriate selection and grown

to OD_{600} ~0.6. The cultures were washed with 10 ml ice-cold LB twice to remove the antibiotic
380 and finally resuspended in 1 ml ice-cold LB. 500 µl of the *E. coli* cell suspension was mixed with 20 µl of *S. venezuelae* spores by inversion and then pelleted by centrifuging at 15,871 xg for 2 minutes. The supernatant was removed, and the pellet resuspended in 150 µl residual supernatant. Serial 10-fold dilutions were plated on SFM and incubated at room temperature for 16-20 hours, overlaid with 1 ml sterile distilled H_2O containing appropriate selection and then incubated at 30°C for 3-7 days until colonies appeared. Colonies were re-streaked on SFM agar with appropriate selection at least once before being plated for spore preparation.

Generation of *S. venezuelae* strain M1702

Deletion of the chloramphenicol biosynthetic gene cluster (BGC) and jadomycin BGC was
390 achieved using the meganuclease system [45]. The upstream flank for the chloramphenicol BGC was amplified with oligonucleotides NH112ChlPCR1F and NH115ChlPCR2R, whereas the upstream flanking of the jadomycin cluster was amplified with NH120JadPCR1F and NH123JadPCR2R. The upstream flanking sequences were then cloned into the BglII and HindIII sites of pIJ12738 [45]. The downstream flanking sequence of the chloramphenicol BGC was amplified with oligonucleotides NH116ChlPCR3F and NH119ChlPCR4R, whereas the upstream flanking sequence of the jadomycin BGC was amplified with NH124JadPCR3F and NH127JadPCR4R. The downstream flanking sequences were combined with the corresponding upstream flanking sequences in pIJ12738 by cloning into the HindIII and SpeI sites. These pIJ12738 derivatives containing the flanking sequencing to each cluster followed
400 by a I-SceI meganuclease cut site were then mobilised via conjugation through *E. coli* ET12567/pUZ8002 and single crossover recombinants were selected for with apramycin. We then conjugated pIJ12742 containing the meganuclease into the single crossover recombinants. Expression of the meganuclease results in a double strand break, which can be resolved by a second crossover event. Subsequent double crossovers were screened by PCR to determine if they were gene cluster deletion mutants or if they had reverted to wildtype. Gene cluster deletion mutants were incubated at 37°C for two generations to promote loss of pIJ12742. The resulting strains were Δ*cml* (M1700) and Δ*jad* (M1701). M1700 was used as the starting material to introduce the jadomycin BGC deletion derivative of pIJ12738, and single crossover recombinants were used to introduce the meganuclease (on pIJ12742)
410 followed by screening for loss of the jadomycin BGC and removal of the plasmid, generating the final double mutant of Δ*cml*Δ*jad* (M1702).

Antimicrobial bioassays

5 µl of spores of the relevant *S. venezuelae* strains were inoculated onto the centre of a YP or YPD agar plate and incubated for 5 days at 30°C. The *B. subtilis* indicator strain was grown in 10 ml LB at 37°C with 220 rpm shaking the night prior to the assay. Following overnight incubation, the indicator strains were sub-cultured 1:100 into 50 ml LB and grown to OD_{600} ~0.6. and then diluted 1:10 into 50°C Soft LB agar. 5 ml of this inoculated soft agar was then

pipetted over the *S. venezuelae*-containing plate ensuring complete coverage. The plates
420 were air-dried and subsequently incubated at 37°C overnight before imaging.

Biomass and glucose quantification assays

5 µl of spores of the relevant *S. venezuelae* strains were inoculated on cellophane-covered YP or YPD agar plates for 5 days at 30°C. Following incubation, the cellophane disks were removed, and the mycelial mass was measured using an analytical balance. For glucose extraction the underlying agar was chopped into small pieces using a sterile scalpel and transferred to a 250 ml conical flask. 20 ml sterile distilled H_2O was added, and samples were incubated for 2 hours at 25°C with shaking at 220 rpm. The resulting liquid was aspirated from the flask and diluted 1:1000 with sterile distilled H_2O before being assayed using the Glucose
430 (GO) Assay Kit (Sigma Aldrich) following manufacturer's instructions.

Chromatin immunoprecipitation followed by sequencing (ChIP-Seq)

5 µl of spores of the relevant *S. venezuelae* strains were inoculated onto cellophane-covered YP or YPD agar plates in triplicate and grown for 5 days at 30°C. To cross-link proteins to DNA the cellophane disks were removed and submersed in 10 ml fresh 1% (v/v) formaldehyde solution at room temperature for 20 minutes. Following a 5-minute incubation in 10 ml 0.5 M glycine solution the mycelium was harvested and washed twice with 25 ml ice-cold PBS (pH 7.4) before being flash frozen in liquid nitrogen and stored at -80°C. For lysis, the pellets were resuspended in 2 ml lysis buffer (10 mM Tris-HCl pH 8.0, 50 mM NaCl, 10 mg/ml lysozyme,
440 EDTA-free protease inhibitor) before 750 µl was transferred to a 2 ml microcentrifuge and samples incubated at 37°C for 30 minutes. For fragmentation 750 µl IP buffer (100 mM Tris-HCl pH 8.0, 250 mM NaCl, 0.5% v/v Triton X-100, 0.1% SDS, EDTA-free protease inhibitor) was added and samples sonicated on ice at 50 Hz for 20 cycles of 10 seconds with at least 1 minute of rest between each cycle. 25 µl of the crude lysate was combined with 75 µl TE Buffer (10 mM Tris-HCl pH 8.0, 1 mM EDTA) and extracted with 100 µl phenol:chloroform. 2 µl of 1 mg/ml RNase A was combined with 25 µl of the resulting extract, incubated at 37°C for 30 minutes and run on a 1% agarose gel to confirm a smear centred at 500 bp. The remaining crude lysate was centrifuged for 15 minutes at 15,871 xg at 4°C and supernatant saved. 750 µl of α-FLAG M2 magnetic beads (Sigma Aldrich) were washed in 3.75 ml 0.5% IP buffer (IP
450 buffer - 150 mM NaCl, 1% Triton X-100, 50 mM Tris-HCl (pH 8.0), 2 mM EDTA, and Roche cOmplete™, Mini, EDTA-free Protease Inhibitor Cocktail tablet(s)) to prepare for them binding. The bead slurry was then mixed with 40 µl clarified lysate and incubated overnight on a vertical rotator at 4°C. The lysate was removed, and the beads washed four times with 500 µl 0.5 IP buffer with 10 minutes vertical rotation at 4°C each cycle. Washed beads were incubated in 100 µl elution buffer (50 mM Tris-HCl pH 7.6, 10 mM EDTA, 1% SDS) overnight at 65°C. Eluant was removed and saved before an additional 50 µl elution buffer was added and incubated at 65°C for a further 5 minutes. Once removed 3 µl of 10 mg/ml proteinase K was added to the combined eluants and incubated at 55°C for 2 hours. DNA was extracted with 200 µl phenol:chloroform and purified using a QIAquick PCR Purification Kit (QIAGEN)

460 following the manufacturer's instructions. DNA was eluted in 50 µl Buffer EB (10 mM Tris-HCl pH 8.5) and 47 µl snap frozen in liquid nitrogen and stored at -80°C. The remaining 3 µl of sample was used to determine the DNA concentration and quality. The Qubit Fluorometer 2.0 with the high-sensitivity kit was used for DNA concentration whilst DNA purity was quantified using a Nanodrop™ 2000 UV-Vis Spectrophotometer. The stored DNA samples were the shipped to Novogene on dry ice for sequencing using the NovaSeq 6000 Sequencing System (Illumina). Raw sequencing data were received as FASTQ files from Novogene and processed as described previously [13]. Raw files were aligned to the *S. venezuelae* NRRL B-65442 genome and enrichment normalised to a moving window of 30 nucleotides compared to a region of the surrounding 3000 nucleotides with the window moving in steps of 15
470 nucleotides.

Protein overexpression and purification

Protein preparation for ReDCaT SPR was performed as follows. N-terminally 6xHis-tagged CutR was expressed from the plasmid pET28a in *E. coli* Rosetta (BL21 DE3) pLysS competent cells. Overnight culture (40 ml) was used to inoculate 4 L of LB with selective antibiotics. Cultures were incubated at 37°C with shaking at 220 rpm until OD_{600}~0.6 before isopropyl-β-D-1-thiogalactopyranoside (IPTG) was added to a final concentration of 1 mM. Cultures were incubated for a further 4 hours then the cells were pelleted by centrifugation and stored at -80°C. Cell pellets were defrosted on ice for 30 minutes before being resuspended in 25 ml
480 lysis buffer (20 mM Tris-HCl pH 8.0, 75 mM NaCl, 0.1% Triton X-100, 10 mg/ml lysozyme, EDTA-free protease inhibitor) and incubated at room temperature for a further 30 minutes. Suspensions were sonicated on ice 8 times at 50 Hz for 30 seconds per cycle with 1 minute off between each sonication cycle. Cell debris was removed by centrifugation at 20,600 xg for 30 minutes at 4°C and the supernatant filtered through a sterile 0.22 µm filter (Sartorius). Clarified lysate was loaded onto a 1 ml HisTrap HP column (Cytiva) pre-equilibrated with Buffer A (50 mM Tris-HCl pH 8.0, 200 mM NaCl, 5% glycerol). The loaded column was washed with increasing concentrations of imidazole (step 1: 10 mM; step 2: 20 mM; step 3: 30 mM) before the protein was eluted using 500 mM imidazole, all in the same buffer. Desired protein fractions were pooled and loaded onto a preparative-grade HiLoad 16/600 Superdex 200 pg
490 gel filtration column (GE Healthcare) pre-equilibrated with gel filtration buffer (50 mM Tris-HCl pH 8.0, 200 mM NaCl, 10% glycerol, filtered). Desired fractions were identified and analysed for purity via SDS-PAGE before being pooled. Aliquots were flash frozen in liquid nitrogen and stored at -80°C.

Reusable DNA Capture Technology Surface Plasmon Resonance (ReDCaT SPR)

Protein-DNA binding site scanning and footprinting was performed using ReDCaT SPR as previously described [23]. Preliminary scanning was performed using promoter regions of interest divided into a series of overlapping double stranded oligonucleotide probes (Supplementary Table 4). The total length of each fragment was 40 bp including 15 bp
500 overlaps. To create the double-stranded probes each fragment was reverse-complimented

and a ReDCaT biotinylated single-stranded linker added to the 3' end as an overhang. For each fragment DNA oligos (IDT) were resuspended to 100 µM in sterile distilled H_2O and 55 µl forward oligo was mixed with 45 µl reverse oligo. Oligos were annealed at 95°C for 5 minutes followed by ramping to 4°C at 0.1°C/s. The annealed DNA fragments were then diluted to a final concentration of 1 µM in HBS-EP+ buffer (150 mM NaCl, 3 mM EDTA, 0.05% v/v surfactant P20, 10 mM HEPES pH 7.4). Positive hits from site scanning were selected for footprinting. 2 bp truncations were made from the 3' end of the selected fragments and similarly from the 5' of the inverted fragment. All ReDCaT SPR experiments were performed using a single Sensor Chip SA (GE Healthcare) on a Biacore 8K SPR system (Cytiva) as follows. For each channel FC_1 was designated as the reference (FC_{REF}) and FC_2 as the test cell (FC_{TEST}). DNA capture at 400 RUs was achieved in FC_{TEST} with a contact time of 60 seconds at a flow rate of 10 µl/min. Protein analyte (Purified CutR; 2 µM or 1 µM) was then added over both FCs for 60 seconds at a flow rate of 50 µl/min followed by a buffer only dissociation of 60 seconds. Regeneration of the chip was achieved using Regeneration buffer (1 M NaCl, 50 mM NaOH) injected for 60 seconds at a flow rate of 10 µl/min over both FCs. All experiments were run in duplicate and data analysis was performed using the Biacore Insight Evaluation software (Cytiva) and Microsoft Excel.

Tandem Mass Tagging proteomic analysis

5 µl of spores of the relevant *S. venezuelae* strains were inoculated on cellophane-covered agar plates as triplicate spots in duplicate. After 2- or 9-day incubation at 30°C the mycelium was scraped off the cellophanes into a 15 ml falcon and resuspended in 10 ml cell lysis buffer (50 mM TEAB buffer pH 8.0, 150mM NaCl, 2% SDS, EDTA-free protease inhibitor, PhosSTOP phosphatase inhibitor). The suspension was disrupted via French press three times before being boiled at 100°C for 10 minutes. Samples were sonicated at 50 Hz four times for 20 seconds per cycle and then pelleted at 3,220 xg for 30 minutes. Protein concentration was determined using the BCA assay (Thermo Fischer Scientific) and 1 mg of protein from each sample transferred to a fresh 15 ml falcon tube. The proteins were precipitated from the supernatant with chloroform-methanol [46] and washed with acetone.

The air-dried pellets were dissolved in 50-100 µl of 2.5% sodium deoxycholate (SDC; Merck). After quantification by BCA assay, 100 µg of protein was reduced, alkylated, and digested with trypsin in the presence of 0.2 M EPPS buffer (Merck) and 2.5% SDC according to standard procedures. After digestion, the SDC was precipitated by adjusting to 0.2% TFA, and the clarified supernatant subjected to C18 solid phase extraction (SPE; OMIX tips; Agilent). Tandem mass tagging (TMT) labelling was performed using a Thermo TMT10plex™ kit (lot TL274393) according to the manufacturer's instructions with slight modifications; the dried peptides were dissolved in 90 µl of 0.2 M EPPS buffer/10% acetonitrile, and 200 µg TMT10plex reagent dissolved in 22 µl of acetonitrile was added. Samples were assigned to the TMT channels in an order avoiding channel leakage between different samples, if possible, as detailed by Brenes et. al [47]. After labelling, aliquots of 1.7 µl from each sample were combined

and analysed on the mass spectrometer (detailed below) to check labelling efficiency and estimate total sample abundances. The main sample aliquots were then combined correspondingly and desalted using a 50 mg C18 Sep-pak cartridge (Waters). The eluted peptides were dissolved in 500 µl of 25 mM NH_4HCO_3 and fractionated by high pH reversed phase HPLC. Using an ACQUITY Arc Bio System (Waters), the samples were loaded to a Kinetex® 5 µm EVO C18 100 Å LC Column 250 x 4.6 mm (Phenomenex). Fractionation was performed with the following gradient of solvents A (water), B (acetonitrile), and C (25 mM NH_4HCO_3) at a flow rate of 1 ml/min: solvent C was kept at 10% throughout the gradient; solvent B: 0-5 min: 5%, 5-10 min: 5-13% curve 5, 10-70 min: 13-40%, 70-75 min: 40-50%, 75-80%: 50-80%; followed by 5 min at 80% B and re-equilibration to 5% for 24 minutes. Fractions of 1 ml were collected, dried down, and concatenated to produce 20 final fractions for MS analysis. Aliquots of 30-40 µl were removed and stored at -80°C for global proteome quantification. Aliquots of all concatenated fractions were analysed by nanoLC-MS/MS on an Orbitrap Fusion™ Tribrid™ mass spectrometer coupled to an UltiMate® 3000 RSLCnano LC system (Thermo Fisher Scientific). The samples were loaded onto a trap column (nanoEase M/Z Symmetry C18 Trap Column, Waters) with 0.1% TFA at 15 µl/min for 3 minutes. The trap column was then switched in-line with the analytical column (nanoEase M/Z column, HSS C18 T3, 1.8 µm, 100 Å, 250 mm x 0.75 µm, Waters) for separation using the following gradient of solvents A (water, 0.1% formic acid) and B (80% acetonitrile, 0.1% formic acid) at a flow rate of 0.25 µl/min; for global protein analysis: 0-4 min 3% B (parallel to trapping); 4-17 min increase B curve 4 to 14%; 17-80 min linear increase B to 35%; 80-102 min linear increase B to 55% followed by a ramp to 99% B and re-equilibration to 3% B for 23 minutes; for enriched phosphopeptides: 0-4 min 3% B (parallel to trapping); 4-11 min increase B curve 4 to 12%; 11-52 min linear increase B to 43%; 52-61 min linear increase B to 55%, 61-64 min linear increase B to 65%, followed by a ramp to 99% B and re-equilibration to 3% B for 23 minutes. Data were acquired with the following parameters in positive ion mode: MS_1/OT: resolution 120K, profile mode, mass range m/z 400-1800, AGC target 2e5, max inject time 50 ms; MS_2/IT: data dependent analysis with the following parameters: top10 in IT Turbo mode, centroid mode, quadrupole isolation window 1.6 Da, charge states 2-5, threshold 1.9e4, CE=35 , AGC target 2e4, max. inject time 70 ms, dynamic exclusion 1 count/7 s with ±7 ppm, multistage activation on with neutral loss 97.98 Da (for phosphopeptides only); MS_3 synchronous precursor selection (SPS): 10 SPS precursors, isolation window 1.6 Da, HCD fragmentation with CE=65, Orbitrap resolution 50k, AGC target 1.5e5, max inject time 175 ms.

The acquired raw data were processed and quantified in Proteome Discoverer 3.1 (Thermo Fisher Scientific); all mentioned tools of the following workflow are nodes of the proprietary Proteome Discoverer (PD) software. The *Streptomyces venezuelae* (http://strepdb.streptomyces.org.uk/, 7420 entries) protein fasta database was imported into PD adding a reversed sequence database for decoy searches; a database for common contaminants (maxquant.org, 245 entries) was also included. For global protein quantification, the database search was performed using the incorporated search engine

CHIMERYS (MSAID, Munich, Germany). The processing workflow also included spectrum selection, the TopN Peak Filter with 20 peaks per 100 Da, and the reporter ion quantification by most confident centroid (20 ppm). The inferys_3.0.0. fragmentation prediction model was used with fragment tolerance of 0.5 Da, enzyme trypsin with 1 missed cleavage, variable modification oxidation (M), fixed modifications carbamidomethyl (C) and TMT10plex on N-terminus and K. Identifications were calculated for False Discovery Rate (FDR) 0.01 (strict) and 0.05 (relaxed). The results were exported into a Microsoft Excel table including data for normalised and un-normalised abundances, ratios for the specified conditions, the corresponding p-values and adjusted p-values, number of unique peptides, q-values, PEP-values, identification scores from both search engines; FDR confidence filtered for high confidence (strict FDR 0.01) only. Further filtering included removal of contaminants and single unique peptide matches.

Chemical extraction of chloramphenicol from solid media

Two 5 µl aliquots of spore stock were used to inoculate cellophane-covered 30 ml agar plates with *Streptomyces* spp. before incubation at 30°C for 2 days. Subsequently the cellophane was removed. Agar was cut into 1 cm^3 pieces using a sterile razor blade and transferred to a 100 ml Duran bottle. 30 ml of HPLC-grade ethyl acetate was added to the agar, briefly shaken, and left at room temperature for 1 hour. The top 25 ml of the ethyl acetate was then transferred to a sterile 50 ml falcon tube and the sample was dried under vacuum. The sample was then resuspended in 500 µl HPLC-grade methanol and transferred to a 1.5 ml microcentrifuge tube. Insoluble particulates were removed via centrifugation at 15,871 xg for 10 minutes with the uppermost 200 µl of solution transferred to a 2 ml HPLC vial containing a 200 µl glass insert for downstream chloramphenicol quantification.

Chloramphenicol Quantification by High-performance Liquid Chromatography

Analytical HPLC was performed on a 1290 Infinity II LC System (Agilent). A chloramphenicol standard curve was prepared in triplicate with serial dilutions of chloramphenicol in methanol from 1000 – 0.01 µg/ml. Chloramphenicol standards and extracted samples were chromatographed over a Kinetex 2.6 µm XB-C18 110 Å, 100 x 4.6mm column (Phenomenex) eluting with a linear gradient: mobile phase A, 0.1% (v/v) trifluoroacetic acid; mobile phase B, acetonitrile; 0 min, 10%B; 1 min, 10%B; 11 min, 100%B; 13 min, 100%B; 13.2 min, 10%B; 15 min, 10%B; flow rate 1 ml/min; injection volume 10 µL. UV absorbance was measured at 278 nm and the peak area at this wavelength was measured for analysis. The minimum concentration of chloramphenicol that could accurately be detected under these conditions was 0.5 µg/ml.

Quantitative reverse transcription PCR (qRT-PCR)

To perform quantitative RT-PCR (qRT-PCR), *S. venezuale* WT, Δ*cutRS,* Δ*htrA3* and Δ*htrA3* + pIJ10257-*htrB* strains were grown on top of sterilized cellophane discs on YP or YPD agar at 30°C for 8-10 days. Colonies were removed from the cellophanes kept in liquid nitrogen whilst

being crushed using a sterile pestle and mortar on dry ice. Crushed samples were resuspended in 1 ml RLT Buffer (Qiagen) supplemented with 1 % 2-mercaptoethanol. This suspension was added to a QIA-shredder column (Qiagen) with the flowthrough transferred to a new 1.5 ml microfuge tube (leaving the pellet). Then, 700 µl acidic phenol:chloroform was added and the sample incubated at room temperature for 3 minutes, and subsequently centrifuged at 15,871 xg. for 20 min. The resulting upper phase was mixed with 0.5 volumes 95 % ethanol. This was then applied to a RNeasy Mini spin column (Qiagen) and processed following the manufacturer's protocol. The eluant was treated with the Turbo-DNase kit (Invitrogen) followed by a RNeasy mini clean-up kit (Qiagen) both used according to manufacturer's instructions. The samples were then flash frozen in liquid nitrogen for storage at −80°C. RNA was quantified with Nanodrop and Qubit Fluorometer and~1 mg converted to cDNA using the LunaScript RT SuperMix Kit (NEB) as per the manufacturer's instructions, including No-RT control reactions. Primers for each transcript were optimized using serial dilutions of template DNA and checked for efficiency by generating standard curves and calculating as follows: *E=(10slope−1)–1*. Primer sets with an efficiency between 90 and 110 % and within 5 % of each other were selected. qRT-PCR was run using the QuantStudio1 (Applied Biosystems) with Luna Universal qPCR Master Mix according to the manufacturer's guidelines for a 20 µl reaction with 2 µl template cDNA and a final concentration of 0.25 mM of each primer. Controls with no reverse transcriptase were run to ensure the absence of contaminating gDNA. ΔC_T values were normalized to the *hrdB* gene, which encodes the housekeeping RNA polymerase sigma factor.

Phylogenetic analysis

Genomes for use in phylogenetic analysis were obtained from the NCBI database[48], in all cases only complete and 'reference' RefSeq genomes were selected to avoid duplication. The accession numbers for genomes used to generate Figure 6A and 6B are given in Supplementary Information 1 and 2 respectively. Protein sequence alignments were carried out using MAFFT version 7 (mafft --memsavetree --retree 1 –treeout) [49,50]. Aligned sequences were used to produce a maximum likelihood tree using FASTTREE (FastTree -jtt alignment_file > output_tree) [51]. The resulting trees were annotated in Interactive Tree Of Life (iTOL) v7 [52]. Homologues of SvCutS and SvCssS were identified by reciprocal BLAST search, where reciprocal BLAST best hits were used in further analysis.

Protein Sequence Alignments

Protein sequences for alignment were obtained via recipricol blast searches using *S. venezuale* GCF_001886595.1 CutS and CssS as the query sequences. The sequences obtained for CutS and CssS homologues are available in Supplemental information 1.7 and 1.8 respectively. Sequences were aligned with Clustal Omega [53] and visualised in Jalveiw [54].

Data availability

The ChIP-seq data generated in this study have been deposited in the GEO database under the accession code GSE225370. The proteomics data generated in this study have been deposited in the ProteomeXchange database with identifier PXD051851. The genome sequence accession numbers and protein identifiers used to generate the data in Figure 7A and 7B available as Supplementary Information 1 and 2 respectively. Protein identifiers used to generate Supplementary Figure 2 and Supplementary Figure 4 are available as Supplementary Information .

REFERENCES

1. Daniels, R. *et al.* Disulfide bond formation and cysteine exclusion in gram-positive bacteria. *Journal of Biological Chemistry* **285**, 3300–3309 (2010).
2. Landeta, C., Boyd, D. & Beckwith, J. Disulfide bond formation in prokaryotes. *Nat Microbiol* **3**, 270–280 (2018).
3. Darmon, E. *et al.* A novel class of heat and secretion stress-responsive genes is controlled by the autoregulated CssRS two-component system of *Bacillus subtilis*. *J Bacteriol* **184**, (2002).
4. Hews, C. L., Cho, T., Rowley, G. & Raivio, T. L. Maintaining Integrity Under Stress: Envelope Stress Response Regulation of Pathogenesis in Gram-Negative Bacteria. *Frontiers in Cellular and Infection Microbiology* vol. 9 Preprint at https://doi.org/10.3389/fcimb.2019.00313 (2019).
5. Rodríguez, H., Rico, S., Díaz, M. & Santamaría, R. I. Two-Component Systems in *Streptomyces*: Key Regulators of Antibiotic Complex Pathways. http://www.p2cs.org/ (2013).
6. Xie, Y. *et al.* An atlas of bacterial two-component systems reveals function and plasticity in signal transduction. *Cell Rep* **41**, (2022).
7. Grabowicz, M. & Silhavy, T. J. Envelope Stress Responses: An Interconnected Safety Net. *Trends in Biochemical Sciences* vol. 42 Preprint at https://doi.org/10.1016/j.tibs.2016.10.002 (2017).
8. Vicente, R. L., Gullón, S., Marín, S. & Mellado, R. P. The three *Streptomyces lividans* HtrA-Like proteases involved in the secretion stress response act in a cooperative manner. *PLoS One* **11**, (2016).
9. Yan, S. & Wu, G. Proteases HtrA and HtrB for α-amylase secreted from *Bacillus subtilis* in secretion stress. *Cell Stress and Chaperones* vol. 24 Preprint at https://doi.org/10.1007/s12192-019-00985-1 (2019).
10. Gullón, S., Vicente, R. L. & Mellado, R. P. A Novel Two-Component System Involved in Secretion Stress Response in *Streptomyces lividans*. *PLoS One* **7**, (2012).
11. Noone, D. *et al.* Signal perception by the secretion stress-responsive CssRS two-component system in *Bacillus subtilis*. *J Bacteriol* **194**, (2012).
12. Westers, H. *et al.* The CssRS two-component regulatory system controls a general secretion stress response in *Bacillus subtilis*. *FEBS Journal* **273**, (2006).
13. McLean, T. C. *et al.* Evidence of a role for CutRS and actinorhodin in the secretion stress response in *Streptomyces coelicolor* M145. *Microbiology (United Kingdom)* **169**, (2023).

14. Daniels, R. *et al.* Disulfide Bond Formation and Cysteine Exclusion in Gram-positive Bacteria. *J Biol Chem* **285**, 3300 (2009).
15. Gullón, S., Marín, S. & Mellado, R. P. Four thiol-oxidoreductases involved in the formation of disulphide bonds in the *Streptomyces lividans* TK21 secretory proteins. *Microb Cell Fact* **18**, (2019).
16. Thompson, B. J. *et al.* Investigating lipoprotein biogenesis and function in the model Gram-positive bacterium *Streptomyces coelicolor*. *Mol Microbiol* **77**, 943–957 (2010).
17. Schlimpert, S. & Elliot, M. A. The Best of Both Worlds—S*treptomyces coelicolor* and *Streptomyces venezuelae* as Model Species for Studying Antibiotic Production and Bacterial Multicellular Development. *Journal of Bacteriology* vol. 205 Preprint at https://doi.org/10.1128/jb.00153-23 (2023).
18. Chang, H. M., Chen, M. Y., Shieh, Y. T., Bibb, M. J. & Chen, C. W. The cutRS signal transduction system of *Streptomyces lividans* represses the biosynthesis of the polyketide antibiotic actinorhodin. *Mol Microbiol* **21**, 1075–85 (1996).
19. Kim, E. S., Hong, H. J., Choi, C. Y. & Cohen, S. N. Modulation of actinorhodin biosynthesis in *Streptomyces lividans* by glucose repression of afsR2 gene transcription. *J Bacteriol* **183**, (2001).
20. Görke, B. & Stülke, J. Carbon catabolite repression in bacteria: Many ways to make the most out of nutrients. *Nature Reviews Microbiology* vol. 6 Preprint at https://doi.org/10.1038/nrmicro1932 (2008).
21. Romero-Rodríguez, A. *et al.* Carbon catabolite regulation in Streptomyces: new insights and lessons learned. *World J Microbiol Biotechnol* **33**, (2017).
22. Görke, B. & Stülke, J. Carbon catabolite repression in bacteria: many ways to make the most out of nutrients. *Nature Reviews Microbiology 2008 6:8* **6**, 613–624 (2008).
23. Stevenson, C. E. M. & Lawson, D. M. Analysis of Protein–DNA Interactions Using Surface Plasmon Resonance and a ReDCaT Chip. in *Methods in Molecular Biology* vol. 2263 (2021).
24. Fernández-Martínez, L. T. *et al.* A transposon insertion single-gene knockout library and new ordered cosmid library for the model organism *Streptomyces coelicolor* A3(2). *Antonie van Leeuwenhoek, International Journal of General and Molecular Microbiology* **99**, (2011).
25. Rojo, F. Repression of transcription initiation in bacteria. *Journal of Bacteriology* vol. 181 Preprint at https://doi.org/10.1128/jb.181.10.2987-2991.1999 (1999).
26. Bertrand-Burggraf, E., Hurstel, S., Daune, M. & Schnarr, M. Promoter properties and negative regulation of the uvrA gene by the LexA represser and its amino-terminal DNA binding domain. *J Mol Biol* **193**, (1987).
27. Liu, B., Hong, C., Huang, R. K., Yu, Z. & Steitz, T. A. Structural basis of bacterial transcription activation. *Science (1979)* **358**, (2017).
28. Busby, S. J. W. & Browning, D. F. Transcription activation in Escherichia coli and Salmonella . *EcoSal Plus* (2024) doi:10.1128/ECOSALPLUS.ESP-0039-2020/SUPPL_FILE/ECOSALPLUS.ESP-0039-2020-S0001.DOCX.
29. Shi, J. *et al.* Structural basis of three different transcription activation strategies adopted by a single regulator SoxS. *Nucleic Acids Res* **50**, (2022).
30. Hutchings, M. I., Hong, H. J. & Buttner, M. J. The vancomycin resistance VanRS two-component signal transduction system of *Streptomyces coelicolor*. *Mol Microbiol* **59**, (2006).

31. McLean, T. C. *et al.* Sensing and responding to diverse extracellular signals: an updated analysis of the sensor kinases and response regulators of *Streptomyces* species. *Microbiology (Reading)* **165**, 929–952 (2019).
32. Sánchez de la Nieta, R., Antoraz, S., Alzate, J. F., Santamaría, R. I. & Díaz, M. Antibiotic Production and Antibiotic Resistance: The Two Sides of AbrB1/B2, a Two-Component System of *Streptomyces coelicolor*. *Front Microbiol* **11**, (2020).
33. Som, N. F. *et al.* The conserved actinobacterial two-component system MtrAB coordinates chloramphenicol production with sporulation in *Streptomyces venezuelae* NRRL B-65442. *Front Microbiol* **8**, (2017).
34. Hallgren, J. *et al.* DeepTMHMM predicts alpha and beta transmembrane proteins using deep neural networks. *bioRxiv* (2022).
35. Clausen, T., Kaiser, M., Huber, R. & Ehrmann, M. HTRA proteases: Regulated proteolysis in protein quality control. *Nature Reviews Molecular Cell Biology* vol. 12 Preprint at https://doi.org/10.1038/nrm3065 (2011).
36. Reardon-Robinson, M. E. & Ton-That, H. Disulfide-bond-forming pathways in Gram-positive bacteria. *Journal of Bacteriology* vol. 198 Preprint at https://doi.org/10.1128/JB.00769-15 (2016).
37. Viaene, T., Langendries, S., Beirinckx, S., Maes, M. & Goormachtig, S. *Streptomyces* as a plant's best friend? *FEMS Microbiol Ecol* **92**, (2016).
38. Edwards, M. J., White, G. F., Butt, J. N., Richardson, D. J. & Clarke, T. A. The Crystal Structure of a Biological Insulated Transmembrane Molecular Wire. *Cell* **181**, 665-673.e10 (2020).
39. Norman, M. P. *et al.* A Cysteine Pair Controls Flavin Reduction by Extracellular Cytochromes during Anoxic/Oxic Environmental Transitions. *mBio* **14**, (2023).
40. Yang, X. *et al.* Crystal structures of YfiR from Pseudomonas aeruginosa in two redox states. *Biochem Biophys Res Commun* **461**, 14–20 (2015).
41. Feeney, M. A. *et al.* ActinoBase: tools and protocols for researchers working on *Streptomyces* and other filamentous actinobacteria. *Microb Genom* **8**, (2022).
42. Cobb, R. E., Wang, Y. & Zhao, H. High-Efficiency Multiplex Genome Editing of Streptomyces Species Using an Engineered CRISPR/Cas System. *ACS Synth Biol* **4**, 723–728 (2015).
43. MacNeil, D. J. *et al.* Analysis of *Streptomyces avermitilis* genes required for avermectin biosynthesis utilizing a novel integration vector. *Gene* **111**, 61–68 (1992).
44. Larcombe, D. E. *et al.* Sequence and origin of the Streptomyces intergenetic-conjugation helper plasmid pUZ8002. *Access Microbiol* **6**, 000808.v3 (2024).
45. Fernández-Martínez, L. T. & Bibb, M. J. Use of the Meganuclease I-SceI of Saccharomyces cerevisiae to select for gene deletions in actinomycetes. *Sci Rep* **4**, (2014).
46. Wessel, D. & Flügge, U. I. A method for the quantitative recovery of protein in dilute solution in the presence of detergents and lipids. *Anal Biochem* **138**, (1984).
47. Brenes, A., Hukelmann, J., Bensaddek, D. & Lamond, A. I. Multibatch TMT Reveals False Positives, Batch Effects and Missing Values. *Molecular & Cellular Proteomics* **18**, 1967–1980 (2019).
48. Sayers, E. W. *et al.* Database resources of the National Center for Biotechnology Information. *Nucleic Acids Res* **52**, D33–D43 (2024).
49. Katoh, K. & Standley, D. M. MAFFT multiple sequence alignment software version 7: Improvements in performance and usability. *Mol Biol Evol* **30**, 772–780 (2013).

50. Katoh, K., Misawa, K., Kuma, K. I. & Miyata, T. MAFFT: A novel method for rapid multiple sequence alignment based on fast Fourier transform. *Nucleic Acids Res* **30**, 3059–3066 (2002).
51. Price, M. N., Dehal, P. S. & Arkin, A. P. FastTree: Computing Large Minimum Evolution Trees with Profiles instead of a Distance Matrix. *Mol Biol Evol* **26**, 1641–1650 (2009).
52. Letunic, I. & Bork, P. Interactive Tree of Life (iTOL) v6: recent updates to the phylogenetic tree display and annotation tool. *Nucleic Acids Res* **52**, W78–W82 (2024).
53. Madeira, F. *et al.* The EMBL-EBI Job Dispatcher sequence analysis tools framework in 2024. *Nucleic Acids Res* **52**, W521–W525 (2024).
54. Waterhouse, A. M., Procter, J. B., Martin, D. M. A., Clamp, M. & Barton, G. J. Jalview Version 2—a multiple sequence alignment editor and analysis workbench. *Bioinformatics* **25**, 1189–1191 (2009).

Acknowledgements

We would like to thank Professor Mervyn Bibb (John Innes Centre) for his contributions to the conceptualisation and generation of *S. venezuelae* strain M1702. We also thank past and present members of the Hutchings and Wilkinson groups (John Innes Centre) and Dr Alison MacFadyen (The Sainsbury Laboratory) and Professor Tracy Palmer (Newcastle University) for useful discussions. We thank John Innes Centre support services for growth media, glassware, plasticware and waste disposal and Phil Robinson for his photography expertise. This work was supported by the BBSRC doctoral training programme grant BB/M011216/1 (T.C.M.); by the BBSRC-funded Institute Strategic Programme Project BBS/E/J/000PR9790 to the John Innes Centre and by the BBSRC-funded Institute Strategic Program Harnessing Biosynthesis for Sustainable Food and Health (HBio) grant BB/X01097X/1 to the John Innes Centre.

Author Contributions.

Conceptualization – T.C.M. and M.I.H.

Data curation – A.D.M.B., G.C., C.M. and G.S.

Formal analysis – T.C.M., A.D.M.B., G.C., C.M. and G.S.

Funding acquisition– M.I.H. and B.W.

Investigation – T.C.M., A.D.M.B., N.A.H., J.C., G.C., C.M. and G.S.

Methodology – T.C.M., A.D.M.B., G.C., C.M. and G.S.

Project administration – T.C.M., M.I.H. and B.W.

Resources – C.M., G.S., M.I.H. and B.W.

Software – G.C., C.M. and G.S.

Supervision – M.I.H. and B.W.

Validation – T.C.M. and A.D.M.B.

Visualization– T.C.M. and A.D.M.B.

Writing – original draft – T.C.M., A.D.M.B. and M.I.H.

Writing – review and editing – T.C.M., A.D.M.B., G.C., C.M., G.S., B.W. and M.I.H.

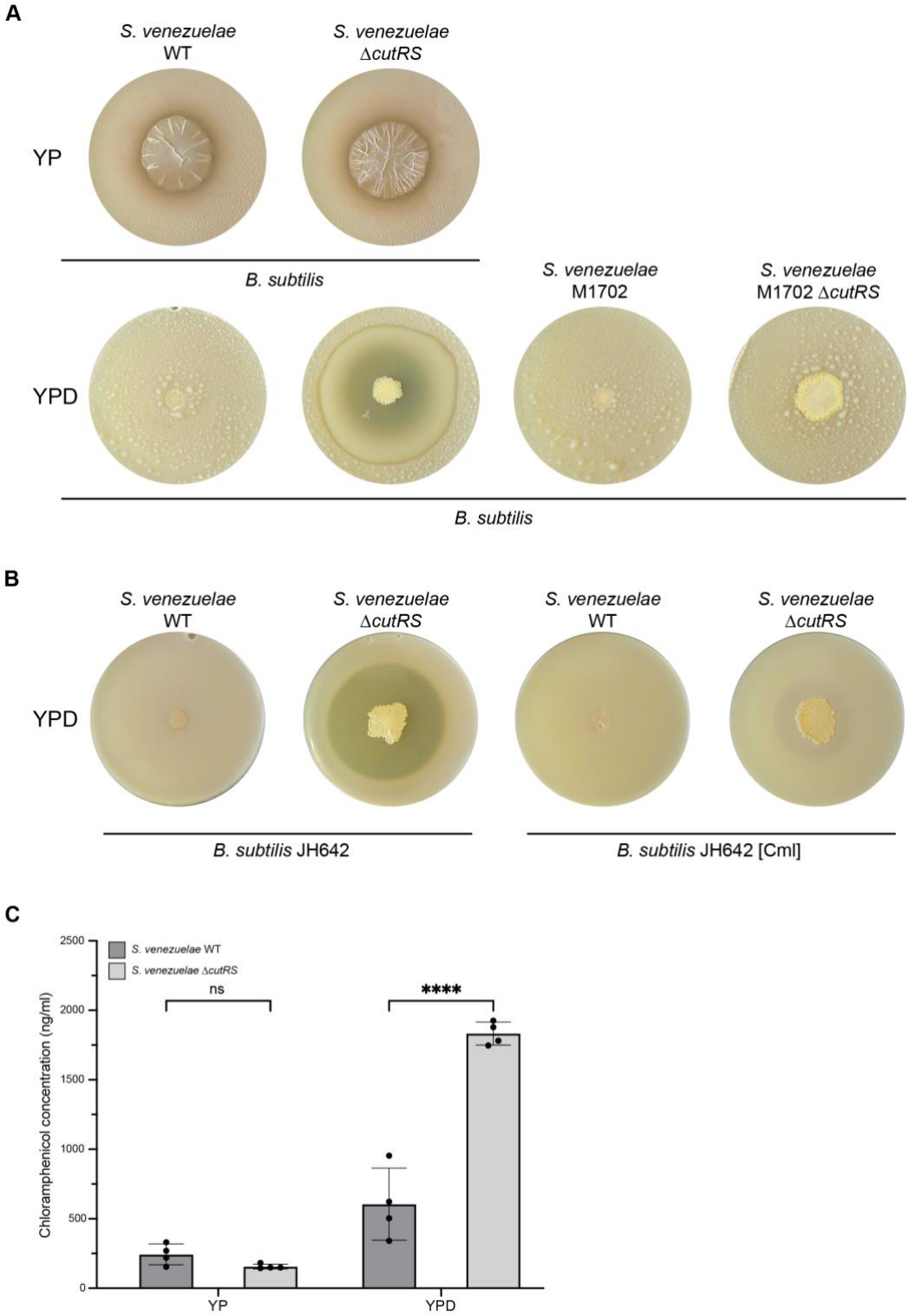

Figure 1. | Deletion of *cutRS* results in the overproduction of chloramphenicol. A. Antimicrobial overlay assays of the *S. venezuelae* WT, Δ*cutRS*, M1702 (Δ*cml*Δ*jad*) and M1702 Δ*cutRS* strains with *B. subtilis.* **B.** Antimicrobial overlay assays of *S. venezuelae* WT and Δ*cutRS* on YPD agar. (left) Overlays with the chloramphenicol-sensitive strain *B. subtilis* JH642. (right) Overlays with the chloramphenicol-resistant strain *B. subtilis* JH642 [Cml]. **C.** Quantification of chloramphenicol extracted from *S. venezuelae* WT and Δ*cutRS* strains on YP and YPD agar by HPLC.

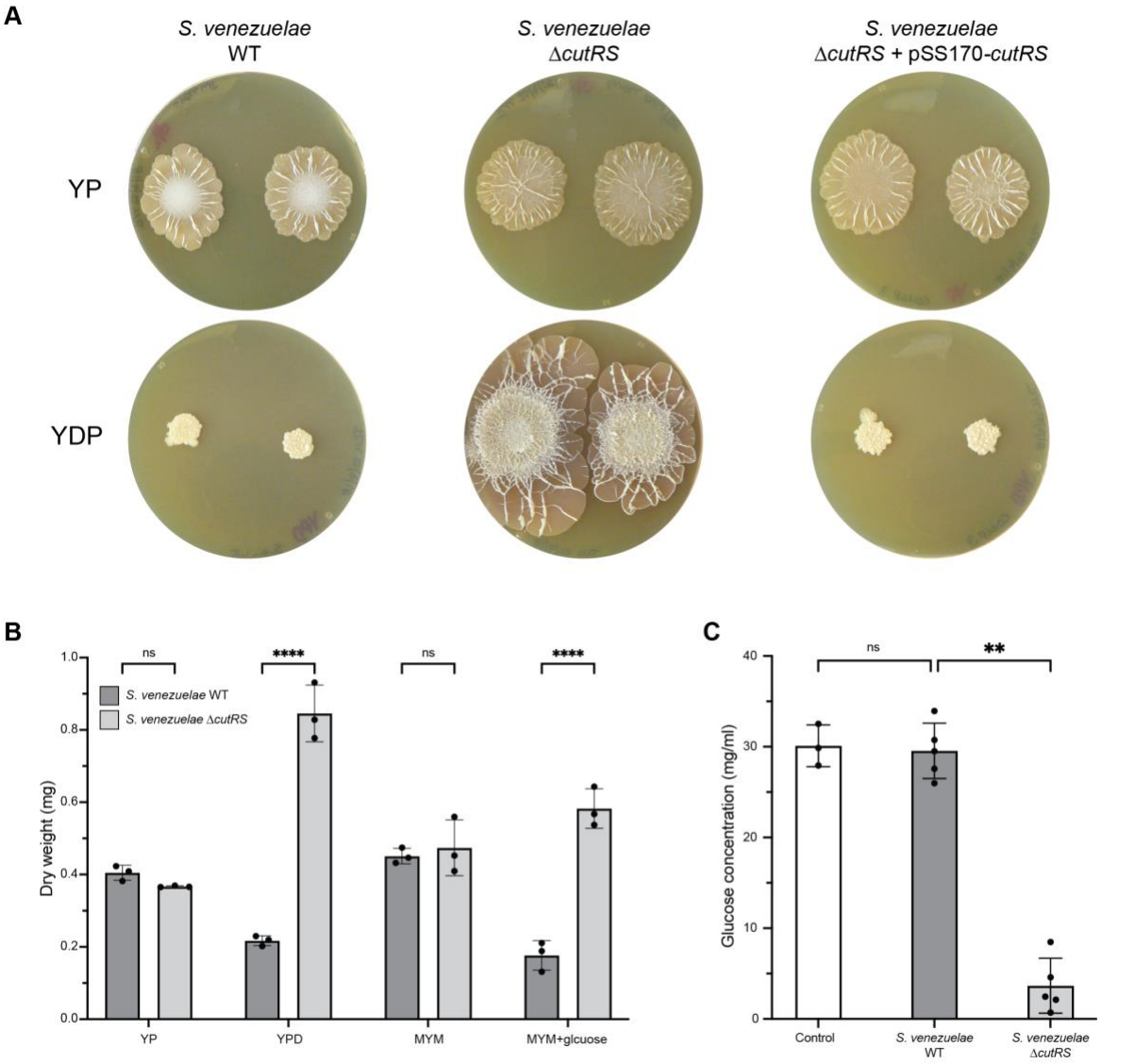

Figure 2. | The CutRS two-component system is involved in colony growth and glucose consumption. A. *S. venezuelae* WT, Δ*cutRS and* Δ*cutRS* +pSS170-*cutRS* colonies grown on YP (- glucose) and YPD (+ glucose) agar for 10 days at 30°C. **B.** The colony dry weight (mg) of *S. venezuelae* WT and Δ*cutRS* after 10 days of growth at 30°C on YP, YPD, MYM and MYM+glucose. **C.** The remaining glucose concentration (mg/ml) in spent media after 10 days of growth at 30°C (*S. venezuelae* WT or Δ*cutRS*).

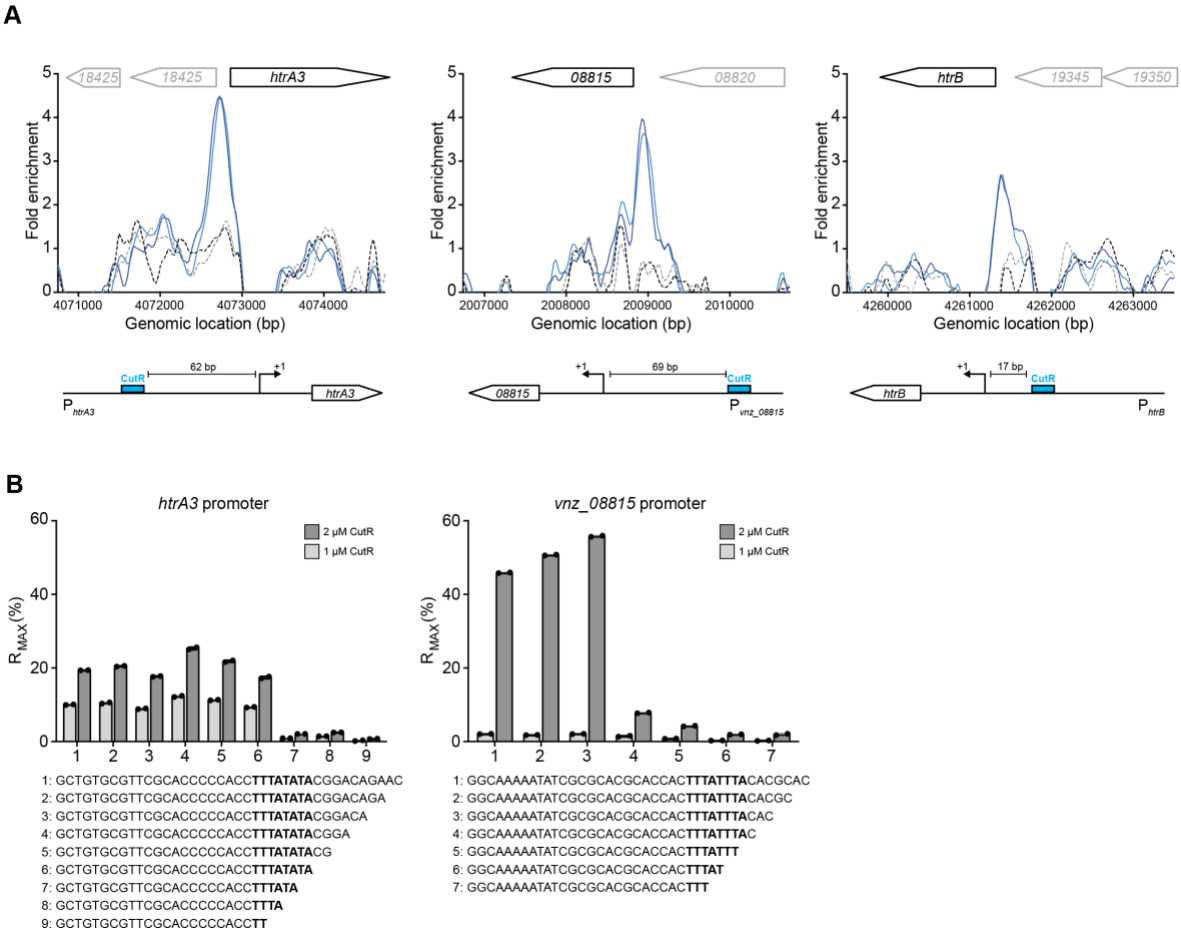

Figure 3. | The defined DNA binding site for the CutR response regulator. A. ChIP-seq peaks for biological replicates of CutR-3xFLAG (blue lines) and the WT control (grey lines). CutR binds upstream of the genes *htrA3*, *vnz_08815* and *htrB.* **B.** ReDCaT SPR was used to determine the binding site of 6xHis-CutR to the promoter regions of *htrA3* and the putative target gene *vnz_08815.* Sequential truncations of 2 bp were used to define the precise binding motif of TAWATAAA. The %R_{MAX} was determined using the molecular masses of the annealed oligo duplex and monomeric 6xHis-CutR. This binding motif was then used to identify the CutR binding site upstream of *htrB* (A).

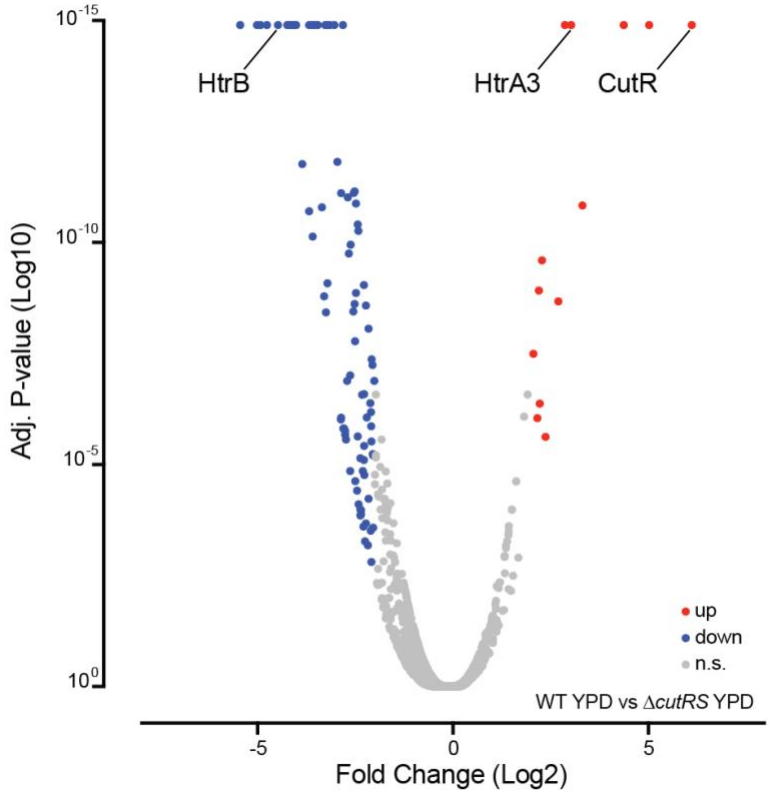

Figure 4. | The deletion of *cutRS* causes a global shift in the proteome. Volcano plot of the Fold Change (Log_2) protein abundance detected by TMT-proteomics against the calculated adjusted P-value (Log_{10}) for *S. venezuelae* wild-type (WT) and Δ*cutRS* strains on YPD agar. The abundance of CutRS in the WT samples appears exaggerated due to the data processing against the Δ*cutRS* samples and does not represent normal levels.

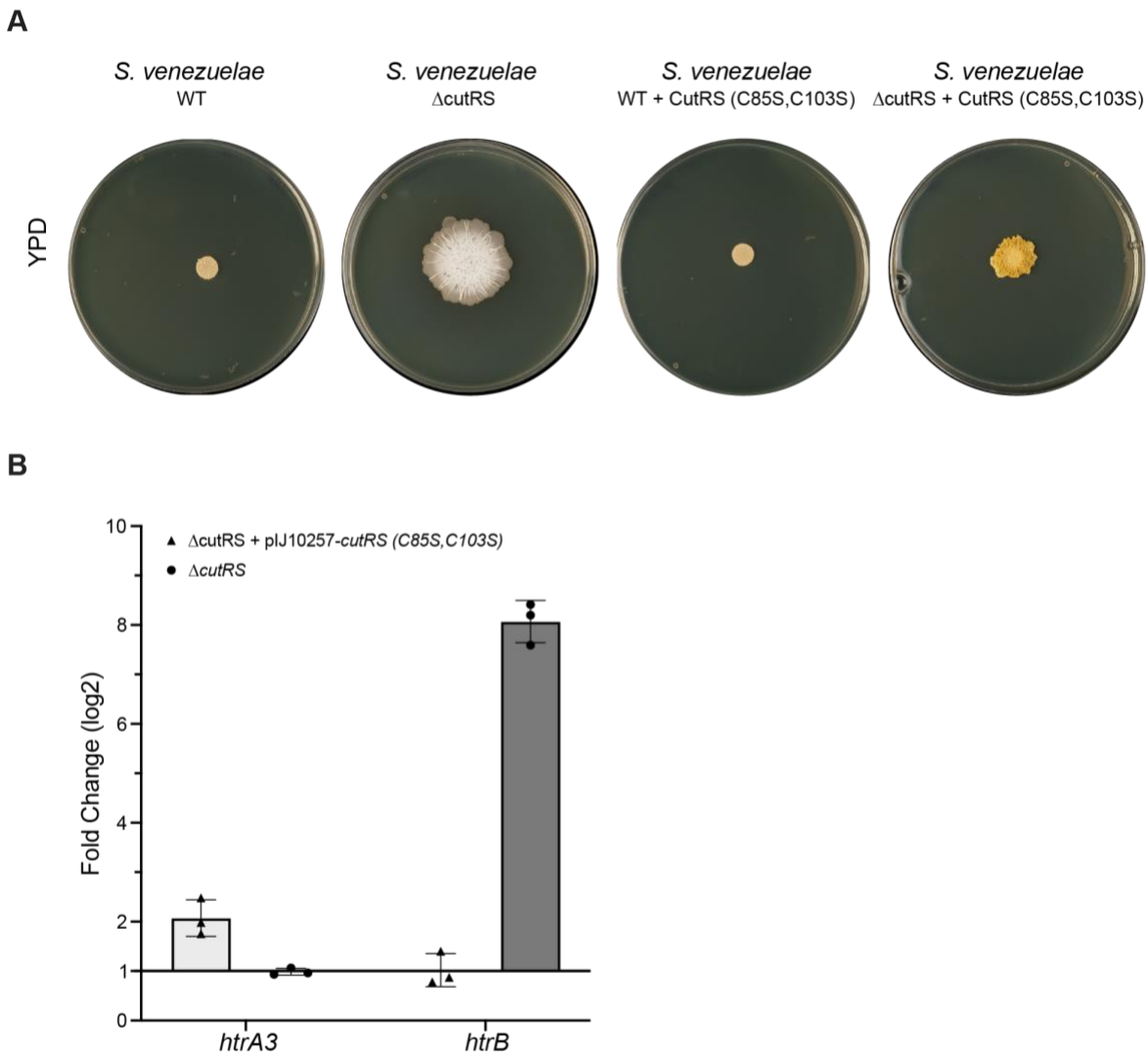

880

Figure 5. | The conserved extracellular cysteine residues control the activity of CutS. A. The Δ*cutRS* mutant can be partially complemented by *in trans* expression of an operon encoding wild-type CutR and a CutS protein in which the extracellular cysteines are altered to serine (CutS(C85S,C103S)). **B.** Quantitative RT-PCR analysing the abundance of *htrA3* (light grey bars) and *htrB* (dark grey bars) transcripts normalised to constitutively expressed *hrdB* and compared to WT. Error bars represent standard deviation across replicates.

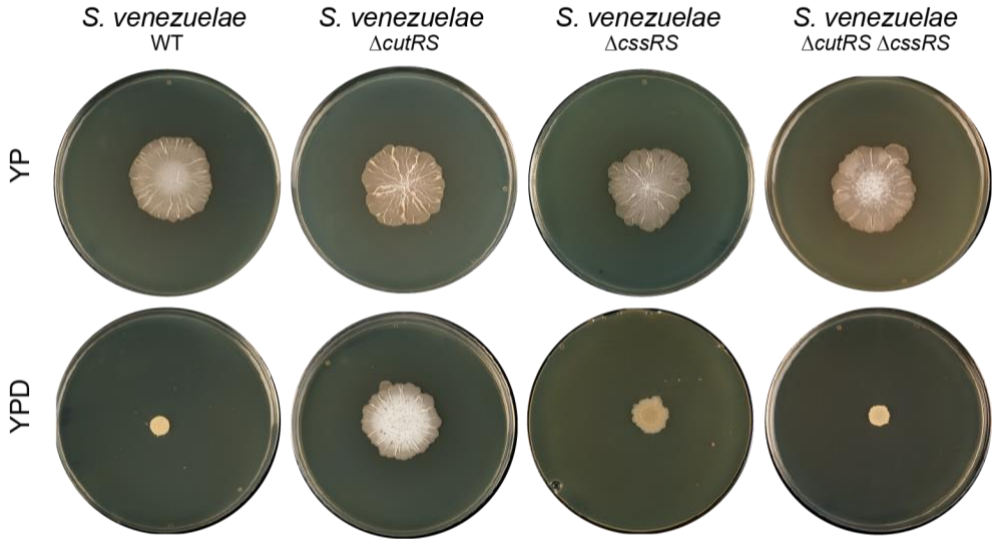

Figure 6. | The *S. venezuelae* wild-type phenotype is recovered by deletion of *cssRS* in the Δ*cutRS* background. *S. venezuelae* WT, Δ*cutRS*, Δ*cssRS and* Δ*cutRS* Δ*cssRS* strains grown on YP (- glucose) and YPD (+ glucose) agar for 10 days at 30°C.

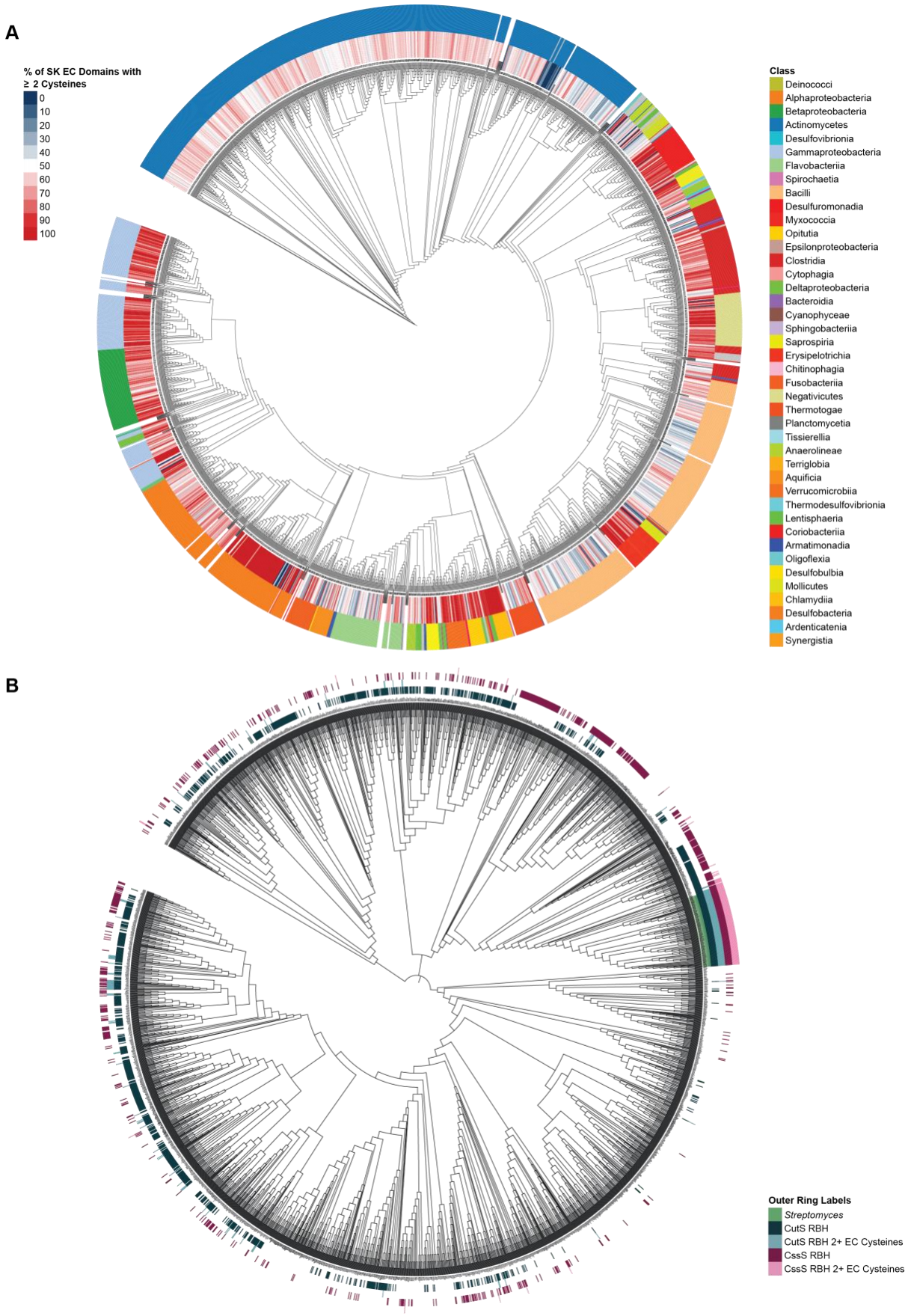
A
% of SK EC Domains with ≥ 2 Cysteines
0
10
20
30
40
50
60
70
80
90
100
Class
Deinococci
Alphaproteobacteria
Betaproteobacteria
Actinomycetes
Desulfovibrionia
Gammaproteobacteria
Flavobacteriia
Spirochaetia
Bacilli
Desulfuromonadia
Myxococcia
Opitutia
Epsilonproteobacteria
Clostridia
Cytophagia
Deltaproteobacteria
Bacteroidia
Cyanophyceae
Sphingobacteriia
Saprospiria
Erysipelotrichia
Chitinophagia
Fusobacteriia
Negativicutes
Thermotogae
Planctomycetia
Tissierellia
Anaerolineae
Terriglobia
Aquificia
Verrucomicrobiia
Thermodesulfovibrionia
Lentisphaeria
Coriobacteriia
Armatimonadia
Oligoflexia
Desulfobulbia
Mollicutes
Chlamydiia
Desulfobacteria
Ardenticatenia
Synergistia
B
Outer Ring Labels
Streptomyces
CutS RBH
CutS RBH 2+ EC Cysteines
CssS RBH
CssS RBH 2+ EC Cysteines

Figure 7. | Phylogenetic and cysteine residue analysis of bacterial sensor kinases. A. Maximum likelihood phylogenetic tree of 348,633 predicted SKs from 12,799 high-quality bacterial genomes. The outer ring is color-coded by bacterial class, as indicated in the legend. The heatmap overlay in the inner ring shows the proportion of SKs with two or more cysteine residues in their extracellular domains, as predicted by DeepTMHMM. Dark blue indicates 0% of the SKs in that genome can form a disulphide bond in their extracellular domain, increasing to dark red, which indicates 100% of the SKs in that genome can form a disulphide bond in their extracellular domain. **B.** Maximum likelihood phylogenetic tree based on RpoB protein sequences from 2,940 bacterial reference genomes. The outer rings represent the following: Genomes in the *Streptomyces* genus (light green); CutS reciprocal BLAST best hits (RBBH) (dark blue); CutS homologs with two or more cysteine residues in their extracellular domains, as predicted by DeepTMHMM (light blue); CssS reciprocal BLAST best hits (RBBH) (dark pink); CssS homologs with two or more cysteine residues in their extracellular domains, as predicted by DeepTMHMM (light pink). Trees were constructed using MAFFT for sequence alignment of RpoB protein sequences and FASTTREE for maximum likelihood inference and visualised in iTOL.

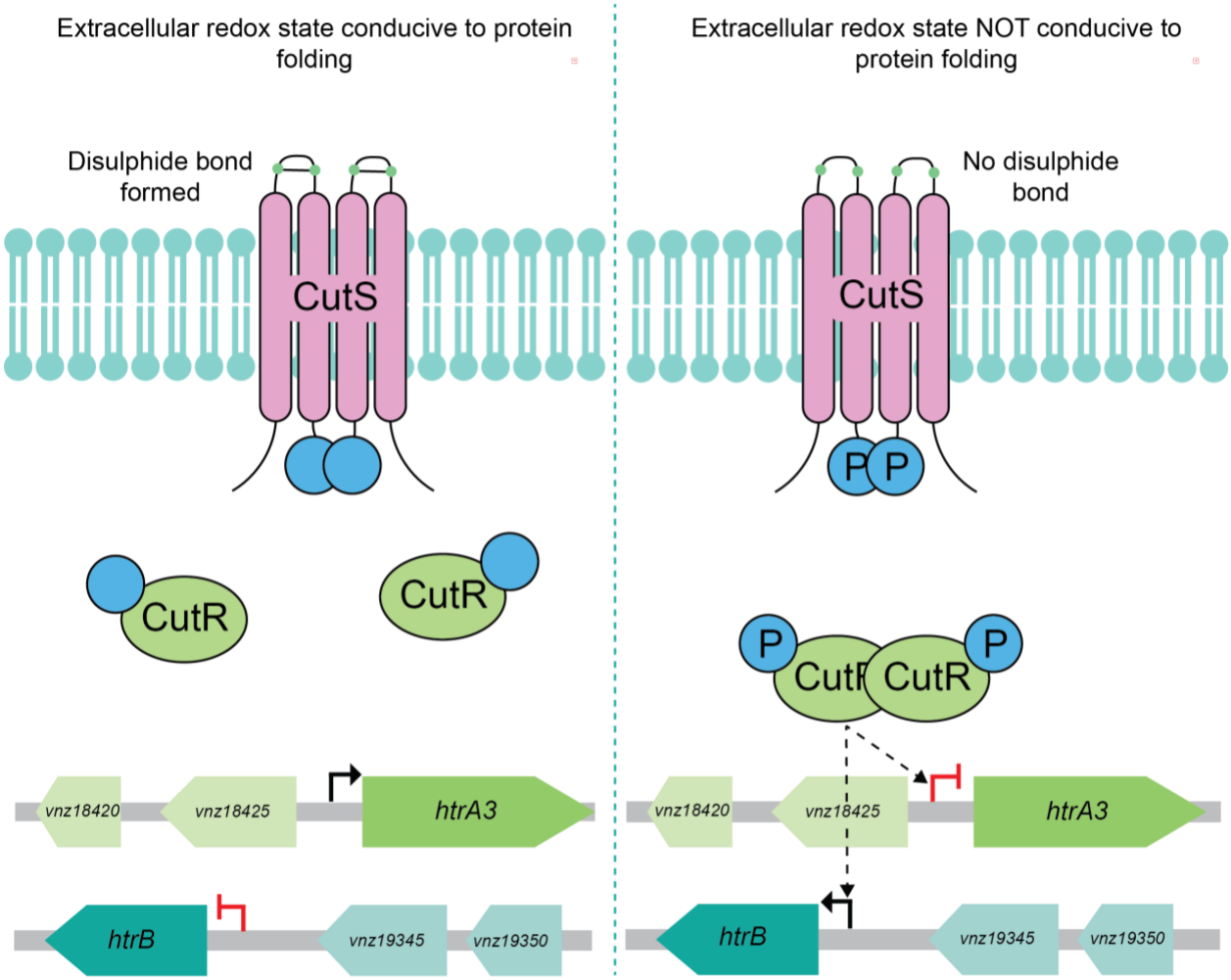

910 **Figure 8. | A proposed model for the extracellular redox-sensing activity of the CutRS system in *Streptomyces* spp.** When the extracellular space is conducive to protein folding (left side) the cysteine residues in the extracellular sensor domain of the SK CutS (pink) form a disulphide bond. In this state the CutRS system is inactive, *htrA3* is expressed and *htrB* is repressed. When the extracellular space in not conducive to protein folding (right side) the disulphide bond in the extracellular sensor domain of CutS is unable to form. In this state the SK CutS is activated, autophosphorylates and transfers this phosphate to the cognate RR CutR (light green). Phosphorylated CutR homodimerises and binds DNA, repressing the transcription of *htrA3* and activating *htrB*. These genes encode dual function chaperone / proteases which can act to restore the cell to homeostasis.

SUPPLEMENTARY FIGURES

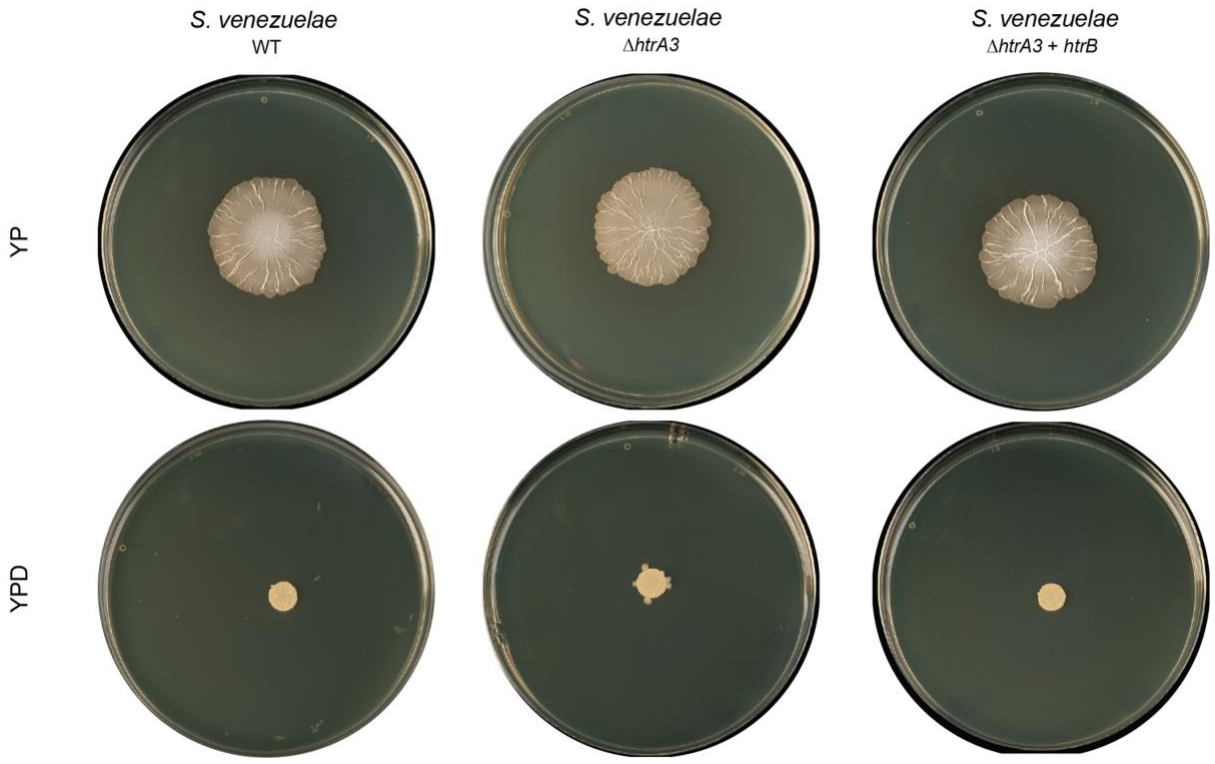

920

Supplementary Figure 1. | Overexpression of *htrB* in the *S. venezuelae* Δ*htrA3* background is unable to reproduce the Δ*cutRS* phenotype. A. *S. venezuelae* WT, Δ*htrA3* and Δ*htrA3* with *htrB* overexpression colonies grown on YP (- glucose) and YPD (+ glucose) for 10 days at 30°C.

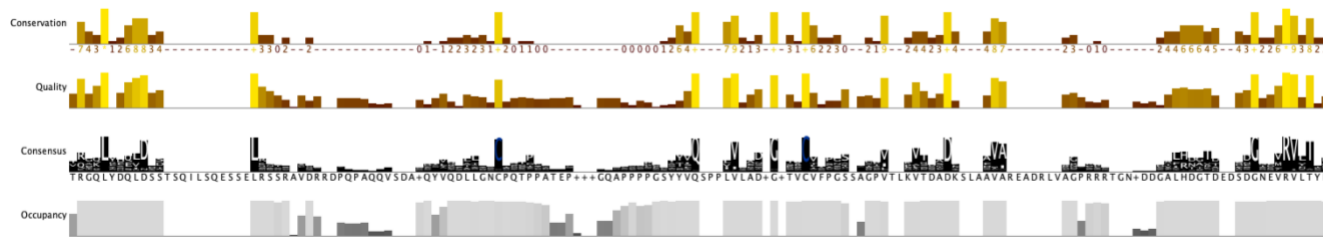

Supplementary Figure 2. | Residue conservation in the extracellular sensor domain of CutS. Clustal OMEGA alignment of 105 CutS homologous from *Streptomyces* spp. showing two highly conserved cysteine residues in the extracellular sensor domain. Alignment view taken from Jalview giving the alignment conservations, quality, consensus and occupancy over one section of the alignment. Sequences use to generate this figure can be found as supplementary file 3.

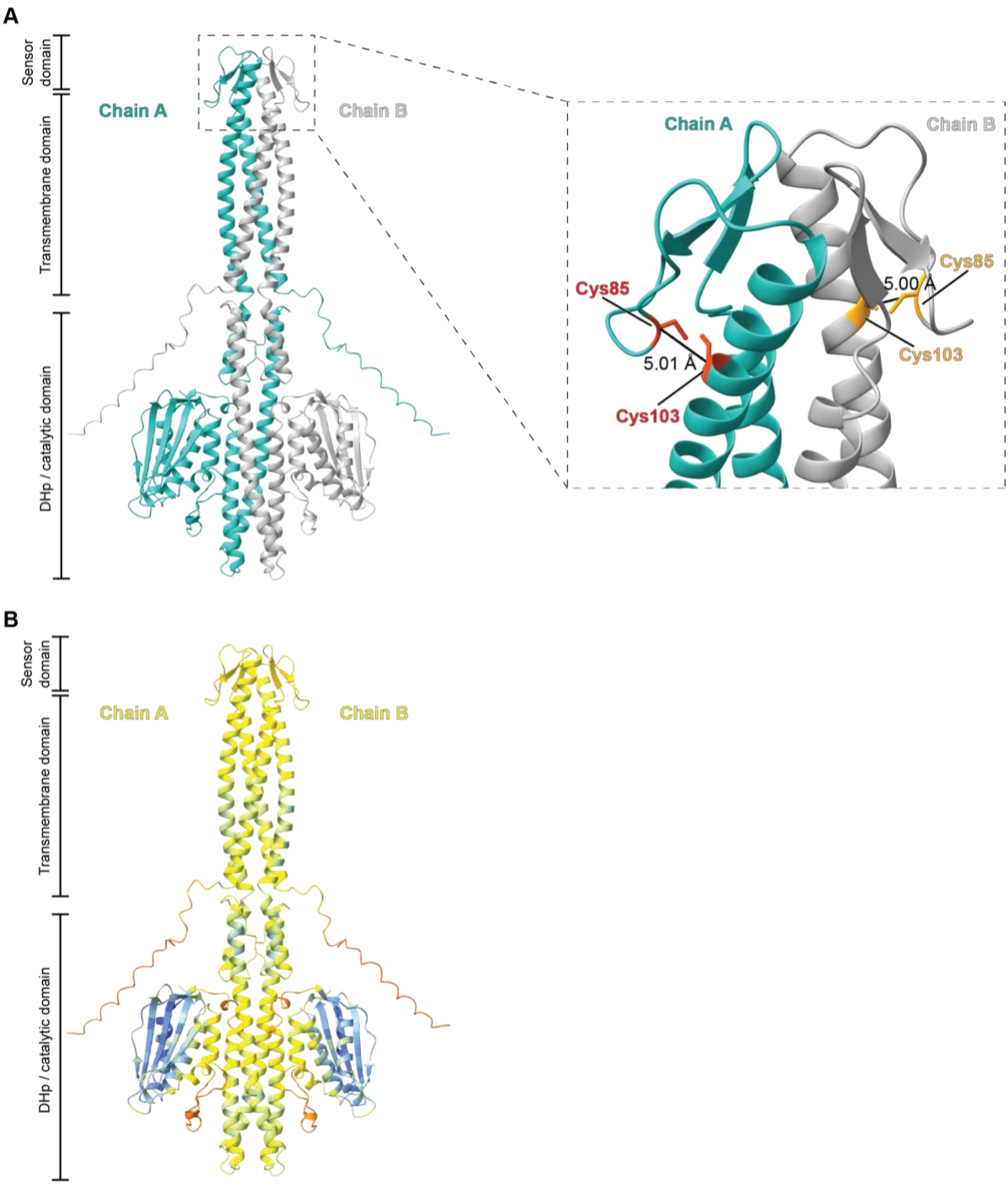

Supplementary Figure 3. | CutS is predicted to form disulphide bonds between the two cysteine residues present in the extracellular sensor domain. A. AlphaFold2-predicted structure of homodimeric *S. venezuelae* CutS. The extracellular sensor domain, transmembrane domain and DHp / catalytic domain are annotated. (Inset) Close-up view of the predicted extracellular sensor domain highlighting the intra-chain disulphide bonds and predicted bond lengths. Chain A: green; Chain B: grey. **B.** AlphaFold2-predicted structure of homodimeric *S. venezuelae* CutS coloured by confidence score (pIDDT): very high (pIDDT > 90; dark blue), confident (90 > pIDDT > 70; light blue), low (70 > pIDDT > 50; yellow) and very low (pIDDT < 50; red).

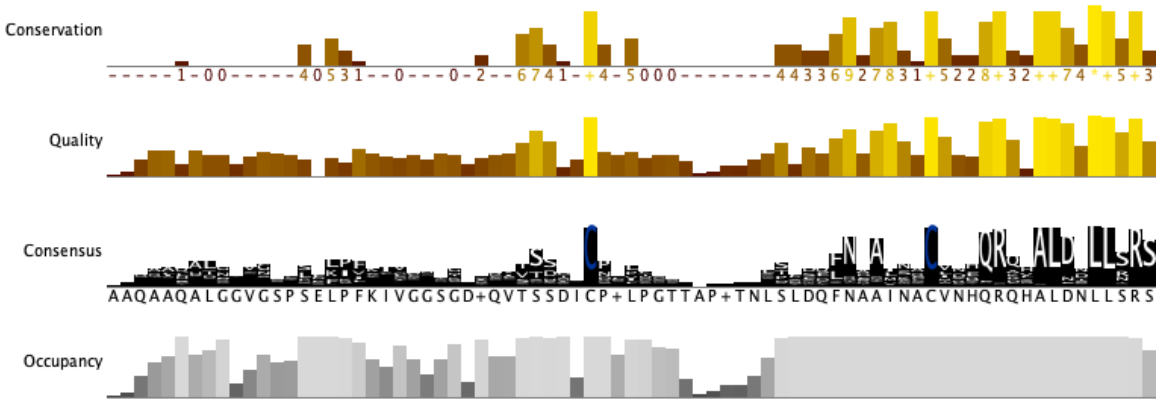

Supplementary Figure 4. | Residue conservation in the extracellular sensor domain of CssS of *Streptomyces* spp. Clustal OMEGA alignment of 105 CssS homologous from *Streptomyces* species showing two highly conserved cysteine residues in the extracellular sensor domain. Alignment view taken from Jalview giving the alignment conservations, quality, consensus and occupancy over one section of the alignment. Sequences use to generate this Figure can be found as Supplementary File 3.

950